NASA TN D-1243

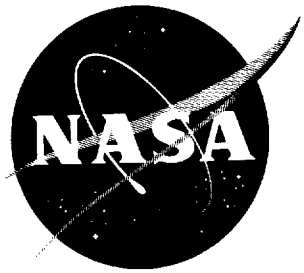

TECHNICAL NOTE

D-1243

DESIGN OF THE NASA LIGHTWEIGHT INFLATABLE SATELLITES FOR THE DETERMINATION OF ATMOSPHERIC DENSITY AT EXTREME ALTITUDES

By Claude W. Coffee, Jr., Walter E. Bressette, and Gerald M. Keating

Langley Research Center
Langley Station, Hampton, Va.

NATIONAL AERONAUTICS AND SPACE ADMINISTRATION

WASHINGTON

April 1962

NATIONAL AERONAUTICS AND SPACE ADMINISTRATION

TECHNICAL NOTE D-1243

DESIGN OF THE NASA LIGHTWEIGHT INFLATABLE SATELLITES FOR THE DETERMINATION OF ATMOSPHERIC DENSITY AT EXTREME ALTITUDES

By Claude W. Coffee, Jr., Walter E. Bressette, and Gerald M. Keating

SUMMARY

A design study has been made of the characteristics of inflatable spheres for use as satellites for determining atmospheric density. The spheres could be fabricated from lightweight material, compactly folded, and inflated to give a large frontal area. The temperature of the inflatable sphere while in a sunlight orbit could be controlled by coating the outside surface of the sphere. A 12-foot-diameter inflatable sphere was successfully injected into orbit and named Explorer IX (1961 Delta 1). The inflatable satellite is optically visible and appears to reflect more like a specular sphere than a diffused sphere. Radar sightings of the satellite have indicated that the 12-foot-diameter satellite is fully inflated.

INTRODUCTION

In order to make accurate predictions of orbital motions and lifetimes of artificial satellites that are relatively close to the earth, the perturbations that affect the orbit must be taken into account. These perturbations (ref. 1, article 1) may include the effect of atmospheric drag, oblateness of the earth, the actions of the heavenly bodies, radiation pressure, and others. The atmospheric drag and the resultant inferred atmospheric density may be obtained from observed changes in the orbital motions of existing satellites (refs. 2 to 5), if the effects of the other perturbations on the orbit are known. However, most of the investigators have cautioned in their reports that the exact value of the atmospheric density obtained by satellite observations is uncertain because the satellites have not been designed specifically for the measurement of atmospheric density. In most cases, the satellites are nonspherical objects and their orientation relative to their velocity vector is not known. Hence, the frontal area and the drag coefficient of the satellite as it passes through perigee must be assumed. The error

in atmospheric density due to the uncertainty in the drag parameter may be of the order of 20 percent. (See refs. 6 and 7.) The lifetime of a satellite is, generally, a direct function of the atmospheric density and the ballistic drag parameter but the lifetime may be affected by other perturbations. The results of the drag exerted by the atmosphere cause the satellite to lose energy continuously during its circuits about the earth. As the satellite energy decreases, the satellite spirals toward the surface of the earth.

In October 1956, a 20-inch-diameter inflatable subsatellite developed by the Langley Research Center was proposed to the United States National Committee for the International Geophysical Year for use in measuring satellite lifetime and therefrom the resultant inferred atmospheric density. The density experiment was approved along with a Naval Research Laboratory magnetometer experiment as satellite experiment package III for the Vanguard launching system. By early 1957, the original 20-inch subsatellite had been enlarged to 30 inches in diameter without any increase in weight because of improved methods of design and construction. These improvements made possible the construction of a 12-foot-diameter inflated sphere weighing approximately 10 pounds. The NASA was then invited to participate in the IGY program with the 12-foot-diameter inflatable sphere using a Department of Defense Jupiter-C launching configuration. During October 1958, the Jupiter-C launching vehicle carrying the 12-foot-diameter inflatable sphere failed to obtain satellite orbit because of a malfunction in the high-speed stages of the configuration. In April 1959, the Vanguard satellite launching vehicle number 5 failed in an attempt to put a 30-inch inflatable sphere in orbit. In August 1959, a second attempt was made to place the 12-foot-diameter inflatable sphere into satellite orbit using a Juno II launching vehicle. This attempt failed because of the loss of guidance of the high-speed stages. A third attempt to place a 12-foot-diameter sphere into orbit during December 1960, by using a developmental Scout launching vehicle, failed. This failure was attributed to a malfunction in the ignition system in which the second-stage rocket motor failed to fire. The fourth attempt made in February 1961, also by using a developmental Scout launching vehicle, was successful in putting a 12-foot-diameter sphere into a satellite orbit.

This paper is concerned primarily with the details of the design and development that lead to the final packages of both the 30-inch inflatable sphere and the 12-foot inflatable sphere systems.

SYMBOLS

All mile dimensions are based on the United States statute mile of 5,280 feet. One United States mile equals 1.609344 kilometers.

a	albedo of earth
A_c	coated surface area of satellite
A_T	total surface area of satellite
c	distance of extreme fiber from elastic axis
C_S	solar constant
D	diameter
h	altitude of satellite
I	moment of inertia of homogeneous section
$k = \frac{R_E}{R_E + h}$	
l	span of beam (diameter of sphere)
n	fraction of composite beam thickness composed of plastic film
q	dynamic pressure
R_E	radius of earth
S	stress in extreme fiber
t	total thickness of beam
T_1	temperature of satellite in sunlight
T_2	temperature of satellite in earth's shadow
α_E	absorbtivity of thermal radiation from earth
α_S	absorbtivity of thermal radiation from sun
ϵ	emissivity
ϵ_i	emissivity of internal skin
ϵ_o	emissivity of external skin
σ	Stefan-Boltzmann constant

Subscripts:

max	maximum
min	minimum
p	satellite coating
u	uncoated satellite

DESIGN PHILOSOPHY

L 1 2 5 1

In considering the design of a satellite specifically for determining satellite lifetime and the resultant inferred atmospheric density, it is necessary to consider some of the physical requirements for this type of satellite.

(1) The satellite should have as large a projected frontal area as possible for the payload weight restrictions of the satellite launching vehicle

(2) The mass of the satellite should be as light as possible within necessary structural requirements

(3) The satellite should be a sphere and retain this configuration without internal pressure for accurate mass to frontal area determination

(4) The satellite should have high reflectivity both in the radio and optical range of the spectrum

(5) The materials of the satellite must be able to withstand the anticipated temperature environment while in orbit

(6) The final design must easily be contained in the payload compartment of the vehicle launching system.

Calculations of the atmospheric density resulting from the measurements of satellite lifetime (refs. 7 to 9) show that the mass of the satellite m, the represented frontal area of the satellite A, and the atmospheric drag coefficient C_D of the satellite must be known. These three quantities, directly associated with the physical properties of a satellite, determine the ballistic drag parameter C_DA/m. The ballistic drag parameter is a direct function of the satellite lifetime

as well as the value of atmospheric density. In the same atmospheric medium a satellite with a large ratio of frontal area to mass will return to earth faster than a satellite having a small ratio of frontal area to mass. In the case of a satellite to be used for measuring satellite lifetime, it would be desirable to obtain measurable reactions on the satellite from the effects of the atmospheric medium within a short time interval. A satellite designed with this in mind, incorporating items 1 and 2 as listed previously, would result in the largest possible size for the weight limitations imposed by the satellite launching system as well as the lightest possible satellite within the necessary structural requirements. However, because an increasingly large ratio of frontal area to mass will result in an increasingly quick return to earth, there exists a lower limit in this design criteria. This lower limit is determined by the capability of being able to acquire the satellite during its return to earth a sufficient number of times so that accurate tracking data are obtained. Therefore, it is important in satellite lifetime measurements to design the vehicle with as large a ratio of frontal area to mass as possible within the limitations imposed on the system by the capability of the tracking equipment.

L 1 2 5 1

Item 3 states that the vehicle to be used for measuring satellite lifetime should be a sphere. A sphere is required for at least two reasons. First, the frontal area of a satellite is a function of the satellite's orientation and the frontal area of a sphere is independent of the satellite orientation. Second, the predicted drag coefficient of a sphere at satellite altitudes should be more accurate because past experience at lower altitudes and speeds has indicated that it is generally easier to predict the drag coefficient for a sphere than for any other shape.

The optical visibility of a satellite that is used for the measurement of lifetime is important because the best optical tracking systems are generally conceded to be superior to electronic tracking systems. (See ref. 10.) The disadvantage of the optical tracking is that the satellite will be visible only during clear weather when the observer is in darkness and the satellite is in sunlight. For good optical tracking, the satellite should be as large as possible and the external shell should have as high a reflectivity as possible in the visible range of the spectrum (item 4). A radio-tracking beacon as well as radar could be employed in conjunction with optical tracking to aid in tracking the satellite during the day and the night. The two tracking systems could be calibrated during the periods of visibility.

The aforementioned requirements have dealt only with the design problems associated with the satellite after it has been placed in orbit. Consideration must also be given to the satellite launching system for the payload weight, orbit capabilities, and compartment size and shape.

INFLATABLE SPHERES

Design and Construction

Configuration.- From the physical requirements given in the section "Design Philosophy," it appears that a highly reflective inflatable sphere would meet the requirements for a satellite drag-measuring vehicle. The sphere can be folded into a compact package and then inflated from this package into shape; thus a large projected frontal area is formed. In this case, the inflated sphere could be made very light for its size because it could be designed in its final form for the small loads that are expected to be encountered in space. The inflatable sphere would resist the heavy loads applied during launching because at this time the sphere would still be a compact package. These capabilities alone do not justify the feasibility of using an inflatable sphere as a satellite drag-measuring vehicle. It also must be demonstrated that such a sphere can be constructed, folded into a compact package, and then inflated to shape while still possessing in its final form the necessary requirements for survival in space long enough to be useful for the determination of atmospheric drag.

Size and weight.- An effort was begun in 1956 at the NACA Langley Laboratory to develop an inflatable sphere that could be compactly folded, inflated in the vacuum of space, and then retain its spherical dimensions in space when the internal gas pressure was released. This effort resulted in the design and construction of both the NASA 30-inch-diameter and 12-foot-diameter spheres shown inflated in figure 1. The 30-inch-diameter sphere was constructed for a total weight of 0.31 pound and it is considered the minimum useful size for a nonradio-instrumented satellite because of the limitations of the optical tracking network in being able to detect it in a satellite orbit. The first 12-foot-diameter spheres each weighed approximately 10 pounds. A lighter inflatable sphere could have been constructed for both sizes shown in figure 1, but it would not have been rigid enough without internal pressure to withstand the anticipated loads in space.

Materials.- The material selected as the gas barrier for construction of the inflatable spheres was a plastic film called Mylar. (See ref. 11.) This material is a very strong lightweight polyethylene film readily available in thicknesses from 1/4 to 5 mils. The plastic film, however, does not satisfy the complete material requirements for an inflatable sphere capable of remaining spherical without internal pressure because it does not possess sufficient compression strength. Therefore, aluminum foil also available in thin sheets (ref. 12) was bonded to the plastic film to give compression strength. The aluminum foil added other qualities, such as increased reflectivity (necessary for optical acquisition of the sphere in a satellite orbit), conductivity

of the sphere surface for radar tracking, and protection of the plastic film which could be affected by ultraviolet radiation. Figure 2 shows the percent loss in weight of the 2-ply laminate (aluminum foil-Mylar) when the two sides were exposed to ultraviolet radiation. The physical properties of the aluminum foil and the Mylar are given in table I.

Fabrication.- The spheres were fabricated by using the conventional balloon-gore type of construction and preformed over a hemispherical mold. Figure 3 shows a completed sphere being removed from the mold by inflation of the sphere. In both the 30-inch-diameter sphere and the 12-foot-diameter sphere, the gores were bonded by using a 3/8-inch overlap between gores. Two adhesives have been used in bonding the gores together; first, Goodyear Pliobond and second, G. T. Schjeldahl Co. GT-301, a thermosetting plastic.

The 30-inch sphere was constructed from composite material consisting of one layer of aluminum, 0.0006 inch thick, laminated to the outside of a layer of plastic film, 0.00025 inch thick. This sphere was fabricated from 36 gores. Since the sphere was to be pneumatically erected, a filling stem was provided for attachment of the inflation bottle.

The 12-foot spheres have been fabricated of two different laminate materials. First, a three-ply laminate consisting of two layers of aluminum foil, 0.00045 inch thick, bonded to a single center layer of plastic film, 0.001 inch thick; and second, a four-ply laminate consisting of alternating layers of aluminum foil, 0.0005 inch thick, and plastic film, 0.0005 inch thick. The spheres were fabricated by using a total of 40 gores. Figure 4 shows some of the construction and material details of the 12-foot inflatable sphere. Figure 4(a) gives the typical gore dimensions used for fabrication and figure 4(c) gives the material and their dimensions used to reinforce the sphere poles at the intersection of gores. Figure 4(e) gives the details of reinforcing the sphere around the pneumatic filler stem to resist the torque loads produced during the inflation of the 12-foot sphere. The torque loads were reduced from their maximum value by a unibal spherical bearing in the filling stem.

Rigidity.- As a first approximation in the determination of the rigidity of the inflatable spheres, a unit width of the sphere was treated as a beam depending essentially upon its local resistance to bending as shown in appendix A. After the sphere fabrication, it was found that the 30-inch spheres were sufficiently rigid to remain spherical without internal pressure as shown in figure 1 and that the 12-foot spheres would remain spherical without internal pressure if supported over the lower hemisphere by a string-weight system as shown in figure 5. The loading placed upon the sphere in this manner is a uniform

loading on the upper hemisphere equal to the weight of the material per square inch. The critical point for buckling was the center of the upper hemisphere where the span was the greatest. This point also corresponded to the point of maximum dynamic pressure on a sphere in a satellite orbit.

The calculated values of dynamic pressure between 50 and 250 statute miles that act upon a satellite spiraling back to earth is presented in figure 6. Also shown for the 12-foot sphere are the design points calculated from appendix A, the ground test point, and the calculated critical buckling pressure for a thin wall sphere under uniform external pressure (ref. 13). The design point was considered to be conservative because it shows that the inflatable sphere will deform at approximately 95 miles whereas the ground test point indicates that the 12-foot sphere could remain spherical without internal pressure to an altitude of about 75 miles and the thin-wall sphere equations indicate approximately 60 miles. If some method of loading was devised to determine the buckling point of the sphere during the ground test, the buckling pressure point for this test in figure 6 would have moved closer to the thin-wall sphere calculation. However, during the static test phase it was evident that the spheres tested were stronger once the aluminum was stressed beyond the yield point.

L 1 2 5 1

Folding and Packaging

Folding methods.- The composite material used in the construction of the inflatable spheres proved to be helpful when the problems associated with packaging were attacked because the sphere could be folded and compressed into reasonable shapes without incurring serious damage to the material. Also, once the folds were made and compressed, the stiffness of the aluminum foil was sufficient to retain the folds in their compressed condition. The principal problem associated with packaging was the removal of the residual air contained inside the sphere. Photographs of the general folding process are shown in figure 7. The bulk of the residual air was removed with a vacuum pump while the sphere was being folded into a basic pleated pattern as shown in figure 7(a). The dimensions and number of pleats depended upon one of the basic dimensions of the compartment that was to contain the folded sphere, such as, the length of a cylinder or the width of a flat compartment.

After pleating and evacuating the residual air, the sphere assumes a flat shape (see fig. 7(b)). The flat shape is folded accordion fashion (fig. 7(c)) so as to form a long, nearly constant width streamer (fig. 7(d)). This streamer can be folded into the desired shape as seen in figure 8, depending upon the shape of the compartment available.

A major consideration other than shape of the compartment and removal of as much residual air as possible was to make all folds in

accordion fashion in order to minimize the possibility of high-pressure gas pockets existing during inflation.

Packaging efficiency.- An idea of the packing efficiency that can be obtained by use of the cylindrical package is shown in figure 8(b). This package was the result of folding a 12-foot-diameter sphere to fit a cylindrical container, 7 inches in diameter and 11 inches long. The total volume of this container was approximately 0.246 cubic foot and the total volume of material in the 12-foot-diameter sphere was approximately 0.0717 cubic foot. This volume relationship gives a packaging efficiency or ratio of material volume to container volume of approximately 30 percent. In other words, the container was still approximately two-thirds full of air. The percentage of this residual air that was contained within the folded sphere was difficult to determine but visual inspection of the packaged sphere within the container indicates that most of the residual air was between the folds and outside of the sphere itself.

Inflation From Complete Package

Inflation system.- The drag loads on the inflatable spheres after being placed in a satellite orbit are many times smaller than the load due to gravity on the surface of the earth where the inflatable spheres were rigid enough to stand by themselves without internal pressure. Because of this, the spheres were designed so as not to maintain their internal pressure after inflation in space. The inflation system, therefore, needed only to eject the packaged spheres from their containers and then inflate the compactly folded sphere to some predetermined stress level and did not have to maintain the internal pressure for any length of time.

Two inflation systems were considered for use in inflating the spheres. The systems were sublimation of either a solid or a liquid in the vacuum of space and a compressed gas system. A major consideration in the selection of the inflation system was the unfolding loads that are inherent in the compactly folded rigid spheres. The pressure required to overcome these unfolding loads may be higher than the final inflation pressure of the fully inflated sphere. The sublimation system will exert a pressure equal only to its equilibrium vapor pressure at a given temperature and if the unfolding loads are greater than the equilibrium vapor pressure, the sphere will not inflate. The compressed gas system when designed for the fully inflated sphere will exert a greater pressure during the unfolding process because of the reduced volume of the folded package. The compressed gas system, as designed, was a simple mechanical system whose reliability could easily be evaluated in vacuum tank tests.

Inflation under atmospheric pressure of some of the early spheres constructed from the laminate indicated that the sphere was more rigid after having been pressurized to the yield stress of the aluminum. The many creases formed on the surface of the sphere during folding were removed when the sphere was inflated to an internal pressure equal to the yield point of aluminum. For the 30-inch-diameter sphere, the internal gas pressure was approximately 0.32 pound per square inch and for the 12-foot-diameter sphere, the gas pressure was approximately 0.1 pound per square inch.

After the final internal pressure of the inflated sphere was known, the size and weight of the inflation bottle could be determined. The capabilities and limitations of the satellite launching system, as well as the size and weight of the inflation bottle, determined the method of injection of the sphere into satellite orbit. The inflation system of the 30-inch inflatable sphere for the Vanguard launching vehicle is given in appendix B and the inflation system of the 12-foot inflatable sphere is detailed in appendix C.

Testing.- During the research and developmental phase of the design of the payloads, many vacuum tank tests were conducted in order to insure the reliability of the design. These tests include ejection of the folded sphere from the container, inflation of the sphere to the desired internal pressure, and separation of the sphere from the inflation system if required. Figure 9 shows the 30-inch sphere after inflation in a vacuum tank and figure 10 shows a 12-foot sphere being inflated in a vacuum. In addition to the tank tests, several vertical probes were made from Wallops Island (refs. 14 and 15).

The complete payloads were subjected to environmental conditions that were expected to be produced by the various launch systems. The environmental conditions include 25g horizontal and vertical vibrations up to 2,200 cycles per second, 100g shock and sustained load, and spin rates up to 1,000 revolutions per minute. After the environmental tests were completed, the payloads were activated in a vacuum tank in order to demonstrate their ability to survive the expected environment without failure.

Decompression tests were made of complete payload packages to determine whether the residual air in the package would cause movement of the folded spheres and affect the dynamic balance of the spinning launch system or prematurely eject the folded 12-foot sphere from the container. Movement of the 30-inch sphere in its package was not considered a problem because of the lightweight of the sphere and because the movement was restrained by the carrier and magnetometer.

The complete 12-foot sphere payload was placed inside of a small decompression tank that, in turn, was connected to a large vacuum as

shown in the sketch included in figure 11. Pressure measurements with time were recorded for the payload package and the decompression tank as the pressure in the decompression tank was rapidly reduced from atmospheric. Two of these tests are presented in figure 10, one a rapid test that lasted for a total of $8\frac{1}{2}$ seconds and a slower test that lasted for 40 seconds. The rapid test $\left(\text{duration, } 8\frac{1}{2} \text{ seconds}\right)$ shows that the pressure inside the payload package lags the decompression tank pressure by 1 to 2 pounds per square inch. This differential pressure could exert a force of approximately 74 pounds on the folded sphere and cause premature ejection. However, a dial indicator located at the forward end of the payload package (fig. 11) during the tests measured a movement of only 0.015 inch. In the slow test (duration, 40 seconds), the leakage of the residual air from the payload package was sufficient to reduce the payload pressure at the same rate as the decompression tank pressure. This slow test was faster than the expected ascent of a Scout vehicle as shown in figure 11. It appears from these tests that premature ejection or dynamic unbalance due to shifting of the payload from residual air does not constitute a problem.

L
1
2
5
1

ESTIMATED ORBITAL CONDITIONS

Lifetime

Estimates of the lifetime of a satellite before being placed into an orbit around the earth are generally erroneous because of certain unknowns that enter into the calculations. These unknowns are generally of three types: first, those that affect the performance of the launching vehicle and the guidance system; second, those that are concerned with the spatial orientation of nonspherical satellite shapes; and third, those that are concerned with the knowledge of the atmosphere at satellite altitudes.

The estimated lifetime of the 12-foot-diameter inflatable sphere is shown in figure 12 for circular and several elliptical orbits. These calculations are based on the change of total energy in an orbit as caused by a drag impulse acting at the perigee altitude (ref. 16) and using the Air Research and Development Command (ARDC) model atmosphere, 1959 (ref. 17). An error is induced into the calculations of the elliptical orbit lifetime by assuming that the perigee altitude does not diminish at all and that the drag impulse is applied only at the perigee altitude. Another error that appears is that the exact atmospheric density at the perigee altitude and exact drag coefficient are not known. These errors may affect the orbital lifetimes by a factor of 10. To

determine the reliability of this estimate of satellite lifetime, it would be necessary to place a sphere of this mass-area ratio (0.00412 slug/ft^2) into orbit. The estimated lifetime from figure 12 for the 12-foot-diameter sphere, weighing 15 pounds, in an elliptical orbit (perigee, 400 miles; apogee, 1,600 miles) is approximately 340 days. Calculation by other methods indicated that the estimated lifetime of the 12-foot-diameter sphere in this orbit would vary from approximately 90 to 520 days. If the mass-area ratio is appreciably increased, the lifetimes become prohibitive. A satellite of the same mass-area ratio as Vanguard I (approximately 0.107 slug/ft^2) would have an estimated lifetime of over 300 years.

Visibility

Because optical tracking of satellites is considered to be more accurate than electronic tracking (refs. 10 and 18) and, also, in case of failure of the satellite's electronic transmitter, optical tracking would be the primary method of satellite acquisition, the degree of optical visibility (stellar magnitude) of the inflated spheres illuminated by the sun while in a satellite orbit had to be determined. In order to predict the optical visibility of the inflatable spheres, it was first necessary to determine whether the spheres reflected diffusely or specularly and what their reflectance or albedo would be.

A small 4-inch-diameter inflatable sphere (fig. 13) was constructed from the material used in the 30-inch-diameter inflatable sphere for the purpose of making reflectivity tests. The small size of the test specimen, dictated by the equipment available for conducting the tests (see ref. 19), was not considered to be detrimental for determining the reflectivity of the larger spheres. The external surface of the 4-inch-diameter sphere (fig. 13) was similar to the external surface of the larger spheres (figs. 1 and 9).

The results of the tests on the 4-inch-diameter inflatable sphere model are presented in figures 14 and 15. In figure 14 is plotted the measured values of sphere-reflected light flux per foot candle of illumination as a function of azimuth angle from the direction of illumination. Also presented in figure 14 are calculated values of the returning light flux as a function of azimuth angle for a diffuse sphere (ref. 20) and for a specular sphere (ref. 21), a unit foot candle being substituted for the solar incident flux and a value of reflectance of 90 percent being used. The distribution of the measured values in figure 14 as compared with the calculated values for specular and diffuse spheres indicates that the inflatable spheres will reflect more like specular spheres than like diffuse spheres. The measured values then were divided by the calculated value for a 90-percent specular 4-inch-diameter sphere to determine the percent reflectance. This value of

reflectance is plotted on a polar coordinate scale in figure 15 as a function of azimuth angle from the direction of illumination. Also presented in figure 15 is the percent reflectivity measured by the same equipment for a machined and polished 4-inch-diameter aluminum sphere. The aluminum sphere was included in figure 15 to show that the scatter in the data is not only inherent in the inflatable sphere but that the surface of the inflatable sphere is comparable to a machined and polished aluminum sphere. An arithmetic average of the measured reflectance points from azimuth angles from 20° to 170° indicates that the inflatable spheres should have an average reflectivity of 79 percent.

L
1
2
5
1

The apparent magnitude at zenith is presented in figure 16 for a specular, 79-percent-reflectivity spherical satellite of 30-inch and 12-foot diameter plotted against distance of satellite from the observer by using the method given in reference 21 for a nighttime sky. Also presented in figure 16 for reference is the magnitude of the Polaris star which is equal in apparent magnitude to the 12-foot-diameter sphere at a distance from an observer of approximately 300 miles. A correction value for atmospheric refraction is presented in figure 16 from the zenith elevation angle of 90° to an elevation angle of 10°.

Thermal Balance

The skin temperatures of the inflatable spheres while in satellite orbits were calculated because the plastic film and the bonding agents used in the lamination of the skin and the fabrication of the spheres would have to withstand these temperatures while in the space environment. These temperature calculations were made on two arrangements of the aluminum foil-Mylar laminate using the equations given in appendix D. The values of emissivity and solar absorptivity used in the calculations are given in table II.

The maximum and minimum skin temperatures in sunlight and in the earth's shadow on the aluminum foil-Mylar inflatable satellite are shown in figure 17 as a function of orbital altitude. Figure 17 shows that by changing the inside surface of the satellite from aluminum foil to Mylar the temperature difference across the satellite is lessened and the difference between the extremes in temperatures is decreased. These results tend to simplify the problem of sustaining the necessary temperature range if electronic components are added to the satellite.

The batteries and transistors included in the electronic components are generally sensitive to temperature and are limited to a temperature range between 60° C and -10° C for satisfactory operation. Because of the low thermal mass of the inflatable spheres, it would be necessary to change the ratio of average absorptivity to emissivity A_s/ϵ_o of the

outside skin of the satellite in order to regulate the maximum skin temperature while in the sunlight. The most applicable method appeared to be coating a percentage of the outside surface with a paint or dye having a lower A_s/ϵ_o ratio than the aluminum surface. Included in figure 17 are the maximum and minimum temperatures, while in the sunlight and the earth's shadow, for an inflatable satellite (outside surface, aluminum; inside surface, Mylar) having 17 percent of the outside surface coated with white epoxy paint. The maximum temperature while in the sunlight has been decreased below 60° C. The temperatures while in the earth's shadow are below those required for satisfactory operation of the electronic components. Therefore, it appears that thermally decoupling the electronic components from the satellite skin is the most satisfactory method of controlling the temperature while in the earth's shadow.

L 1 2 5 1

The maximum temperature to which the spheres were subjected during curing operations after fabrication was approximately 163° C, which, as may be seen from figure 17, is above the maximum skin temperature of the satellite while in the sunlight.

RESULTS AND DISCUSSION

On February 16, 1961, at approximately 13:16 Greenwich mean time (G.m.t.), a 12-foot-diameter inflatable sphere for the measurement of satellite drag and the resultant inferred atmospheric density was injected into orbit. The launching vehicle was the NASA Scout, a four-stage solid-fuel rocket system. The primary consideration of the launching was the continued development of the Scout as a launching system capable of placing a payload into orbit and the secondary consideration of the launching was the payload itself. After obtaining orbit, the inflatable satellite was named Explorer IX (Harvard Observatory Notation 1961 Delta 1).

The Explorer IX satellite, shown in figure 18, was constructed from the four-ply laminate, consisting of alternating layers of aluminum foil and plastic film. The aluminum foil formed the outside surface and the plastic film, the inside surface. Approximately 17 percent of the total outside surface was covered with white epoxy paint to help accomplish the requisite thermal balance on the satellite. In order to upgrade the experiment by providing continuous day and night tracking, the satellite was equipped with a radio tracking beacon. The satellite, as shown in figure 18, was divided at its equator into two hemispheres by means of a dielectric separator in order that the two metal foil hemispheres would serve as the antenna for a tracking beacon. The total orbital weight of the inflatable sphere and tracking beacon components was 14.62 pounds.

The folded sphere was ejected from the payload container, while the container and fourth-stage motor were spinning at approximately 220 revolutions per minute, traveling at a velocity of approximately 26,100 feet per second and was at an altitude of approximately 420 statute miles. The sphere successfully inflated and separated from the container.

The tracking beacon on the satellite was first acquired during the initial orbit by the NASA Minitrack station at Esselen Park, South Africa. The Minitrack station at Woomera, Australia obtained the satellite tracking beacon signal approximately 2 minutes before the satellite entered the earth's shadow and tracked for about 17 minutes while in the shadow. The acquisition of the tracking beacon signal indicated that the folded sphere had inflated successfully because the satellite's skin formed the radio transmitter antenna. The transmitter failed after passing out of range of the Woomera Minitrack station and before coming into range of the next Minitrack station.

The primary tracking facilities were the Smithsonian Astrophysical Observatory (SAO) Baker-Nunn camera stations. The Baker-Nunn camera station, Olifantsfontein, South Africa, first acquired the satellite at 18:05 G.m.t., February 16, 1961. The satellite was next sighted by the Baker-Nunn camera station, Jupiter, Florida at 10:44 G.m.t., February 17, 1961. Over 1,000 sightings of the satellite were reported by the Baker-Nunn camera stations and SAO Project Moonwatch teams; these reports indicated that the satellite gave a steady white light. The stellar magnitude of the satellite against a known star background have agreed with the theoretical predictions for a 12-foot-diameter sphere at the orbital distances involved.

The satellite has been tracked by radar on numerous occasions and the radar cross sections have indicated that the satellite was fully inflated.

The Explorer IX satellite, because of its low ratio of mass to area (0.00402 slug/sq ft) and based on the initial orbit (perigee, 392.8 statute miles; apogee, 1,607.2 statute miles) given by the developmental Scout launching vehicle, should remain in orbit for approximately one year. The major perturbation of the satellite orbit, other than the effect of the oblateness of the earth, appears to be the effects of atmospheric drag and solar radiation pressure. The combined effects of atmospheric drag and solar pressure are making measurable differences in the satellite orbit over short periods of time; thus, the 12-foot-diameter inflatable sphere is a satisfactory instrument for measuring orbital perturbations due to the atmospheric density and solar radiation. An effort is being expended to differentiate between the magnitude of the two effects.

CONCLUDING REMARKS

The design study of the characteristics of inflatable spheres has indicated that such spheres are practical for the use as satellites for determining atmospheric density. The spheres could be fabricated from lightweight material, compactly folded, and inflated to give a large frontal area. A solar-powered radio beacon can be attached to the surface of the sphere. The temperature of the electronic components of the beacon can be controlled within satisfactory operating limits while the spherical satellite is in sunlight by applying a white epoxy paint coating to 17 percent of the outside surface of the sphere. A 12-foot-diameter inflatable sphere, Explorer IX, was successfully ejected from the payload container at an altitude of 420 statute miles while spinning at approximately 220 revolutions per minute and traveling at a velocity of 26,100 feet per second. The aluminum-foil inflatable satellite is optically visible in its orbit and appears to reflect more like a specular sphere than a diffused sphere. Over 1,000 sightings were reported during the first 115 days in orbit and the optical observations have indicated that the satellite gave a steady white light with the stellar magnitude agreeing with predictions for the 12-foot-diameter inflatable sphere. Radar sightings have indicated that the 12-foot-diameter satellite is fully inflated.

Langley Research Center,
National Aeronautics and Space Administration,
Langley Air Force Base, Va., January 30, 1962.

APPENDIX A

DETERMINATION OF MAXIMUM SKIN STRESS WITH SATELLITE ALTITUDE

In the determination of the maximum buckling stress for the inflatable spheres, it was assumed that the thin-wall sphere equations are not valid because of the residual wrinkles in the sphere skin and that rigidity of the spheres will depend upon the local skin stiffness. A further assumption was made that a unit width of the skin could be considered to be a beam that would collapse when the bending moment imposed produces a stress in the extreme fiber equal to or greater than the yield stress of the material in the extreme fiber. The flexure formula (ref. 22) gives the relationship between the bending moment and the yield stress in the extreme fiber. In order to use this formula, it is first necessary to transform the composite material into an equivalent homogeneous material. This transformation may be done by using the ratio of the modulus of elasticity of the two materials. The section modulus of the homogeneous material based on a three-ply laminate consisting of aluminum and Mylar is

$$\frac{c}{I} = \frac{6}{(18.7 - 17.7n^3)t^2} \tag{A1}$$

In a satellite orbit lower than 250 miles, the bending moment will be applied principally by the dynamic pressure, the weight of the material being neglected. The dynamic pressure in this case should act upon the beam with the maximum load at the center and with a minimum load at the ends because of the satellite's spherical shape. By assuming a linear variation between the maximum and minimum loads, the maximum bending moment for a beam triangularly loaded can be obtained in terms of the dynamic pressure per unit width of the beam.

By combining the flexure formula, the section modulus (eq. (A1)), and the maximum bending moment in terms of the dynamic pressure, an expression for the variation of maximum skin stress with satellite altitude can be obtained

$$S = \frac{ql^2}{2(18.7 - 17.7n^3)t^2} \tag{A2}$$

This expression shows that the maximum skin stress in the extreme fiber is directly proportional to the dynamic pressure and the square of the sphere diameter and inversely proportional to the square of the skin thickness and the cube of the fraction of the skin composed of plastic film.

APPENDIX B

30-INCH-DIAMETER INFLATABLE SUBSATELLITE FOR THE VANGUARD LAUNCHING VEHICLE

The 30-inch-diameter subsatellite experiment was approved by the United States National Committee for the IGY, Technical Panel on Earth Satellite Projects, in February 1957 for use with a magnetometer experiment on a Vanguard launching system. The subsatellite was to be Earth Satellite Project number 29.

The arrangement of the magnetometer and the subsatellite package on the last stage rocket is shown in figure 19. Photographs of the subsatellite package are shown in figure 20. The design, construction, and folding process of the subsatellite have been previously discussed. The subsatellite was fabricated from a two-ply laminate consisting of a single layer of aluminum foil, 0.0006 inch thick, bonded to a single layer of plastic film, 0.00025 inch thick.

The inflation bottles were made of 17-4 PH (condition H-1000) stainless steel. Two inflation bottles were designed for use with the subsatellite. One bottle was nondetachable (fig. 21(a)), and the other bottle was automatically detachable from the satellite upon inflation (fig. 21(b)). The purpose of the two systems was that the mass of the orbiting element could be increased approximately 30 percent while the frontal area was increased a maximum of 0.4 percent. The system to be used would be based on the expected lifetime calculated from the orbiting altitude provided by the launching vehicle. The inflation mechanism is shown in figure 22(a) and was the same for both bottles. The system being armed when the arming pin that fixed the trigger to the bottle was pulled. The trigger prevents the piston valve from moving and inflating the sphere. The arming pin was not pulled until after the satellite packages were in place on the launching vehicle and a few hours before launching. After the system was armed, the magnetometer and the subsatellite carrier prevented the trigger from being operative. When the magnetometer was ejected from the third-stage vehicle, the force that fixed the trigger was removed. The piston valve was pushed down by the gas pressure in the bottle and the gas escaped into the folded subsatellite.

The detachable bottle had two latches that firmly gripped the filling adapter of the subsatellite. (See fig. 22(b).) These latches were held in place by pistons utilizing the gas pressure in the bottle. When the pressure in the bottle dropped to approximately 100 pounds per

square inch, the separation spring forced open the latches and allowed the subsatellite to separate from the bottle.

Pertinent characteristics of the two inflation bottles are:

	Weight empty, gm	Volume, cu in.	Operating pressure, lb/sq in.
Nondetachable	60	2.26	2,000
Detachable	78	3.22	1,500

The nondetachable bottle was selected for use with the Vanguard launching vehicle because of the low perigee altitude (350 statute miles) that was anticipated with this launching system.

The inflation gas used was preprocessed nitrogen. Vacuum tank tests indicated that the change from a folded shape to a spherical shape occurred in approximately 2 seconds and was fully inflated in approximately 15 seconds, internal pressure being approximately 0.3 pound per square inch. Using the detachable bottle at 1,500 pounds per square inch, the subsatellite and the bottle separated at approximately 15 seconds.

The subsatellite carrier shown in figure 20 was made of laminated 0.003 glass fiber and an epoxy resin. The carrier was designed to fit between the magnetometer and the third-stage vehicle. (See fig. 19.) An aluminum insert was used at the attachment point because the original all-plastic carrier failed in compression when tightening the attachment bolts and/or in shear when the subsatellite package was subjected to 25g vibration tests.

The foam-rubber spacer shown in figure 20 was used between the magnetometer and the folded subsatellite. This spacer served two purposes, the first was to prevent damage to the subsatellite by the magnetometer and the second was to hold the subsatellite and the inflation bottle firmly in place during flight, and thus prevent the satellite package from becoming unbalanced. The spacer was made as light as possible and still have a maximum of bearing surface.

The approximate weights of the 30-inch subsatellite package are:

Component	Weight, gm
30-inch subsatellite	137
Nondetachable bottle filled with dry nitrogen	65
Carrier	101
Foam-rubber spacer	15
Total weight	318

This weight of 318 grams (approximately 0.7 pound) was the original weight allowed for the subsatellite package.

The magnetometer was to be ejected from the third-stage vehicle by an ejection spring that gave an added velocity of approximately 4 feet per second to the magnetometer. While the magnetometer was separating from the vehicle, the force restraining the trigger on the inflation bottle was being decreased. When this force was removed, the gas loaded piston valve was allowed to open and the pneumatic erection of the subsatellite expelled the subsatellite from its carrier and the third-stage vehicle. Pressure within the subsatellite was to be released through small gas vents. The weight of the orbiting subsatellite and inflation bottle would be approximately 0.44 pound.

APPENDIX C

12-FOOT-DIAMETER INFLATABLE SPHERE PAYLOAD FOR JUPITER-C, JUNO II, AND SCOUT LAUNCHING VEHICLES

The NACA was invited by the United States National Committee for the IGY to participate in the IGY program with a 12-foot inflatable sphere for use as an air drag and density experiment in March 1958. A schematic drawing of the 12-foot-diameter inflatable sphere payload is shown in figure 23. A photograph of the major subassemblies (inflation bottle, ejection bellows, disconnect, and folded 12-foot-diameter sphere) are shown in figure 24.

A drawing of the inflation bottle and the inflation valve mechanism is shown in figure 25. The inflation bottle was made of SAE 4340 steel normalized after welding. The volume of pressure bottle was approximately 102 cubic inches and the operating pressure of the system was 1,500 to 1,800 pounds per square inch. The inflation gas was 0.4 to 0.5 pound of preprocessed nitrogen.

The inflation mechanism consisted of seven basic parts that are as follows:

(1) Inflation bottle which contained the inflation gas required for successful ejection, inflation, and separation of the 12-foot-diameter sphere from its container,

(2) The squib body which contained the two actuating squibs and the piston that was used to open the inflation valve,

(3) Piston snap ring which prevents the piston and valve from closing after firing of the squibs,

(4) The valve body which contains the inflation valve and the gas return port,

(5) The inflation valve that is held in the closed position by the pressure in the inflation bottle,

(6) The gas return tube which connects the gas return port in the valve body to the inflation bellows, and

(7) The fill valve that is used to fill the inflation bottle and is contained in the valve body.

The sequence of operating starts with the firing of the two squibs. Either squib was capable of actuating the inflation mechanism and the simultaneous firing of both squibs did not create pressure sufficient to destroy the mechanism. The pressure from the squibs moved the piston forward against the valve. The valve and piston then travel against the pressure in the inflation bottle until the snap ring expands. The snap ring prevents the pressure in the inflation bottle from closing the valve and also prevents the piston from returning to its original position; the squib explosion gases were thereby allowed to leak out of the vent in the squib body. With the valve open, the inflation gas passes around the valve, through a gas port into the gas return tube, and out into the ejection bellows.

A drawing of the ejection bellows is shown in figure 26. The bellows were made in three parts: (1) the flexible bellows were made of Fairprene; (2) the sliding piston on the forward end of the bellows was made of aluminum and was an attachment point for the disconnect mechanism (fig. 27); and (3) a laminated glass fiber bulkhead that was attached to the inflation bottle by flat-head screws. The flexible bellows were packed inside the aluminum piston and the glass fiber bulkhead.

Upon opening of the valve in the inflation bottle, the nitrogen gas escaped into the bellows and expanded them almost instantaneously. The expansion was restrained radially by the payload container; thereby, the bellows were forced to expand longitudinally. The longitudinal expansion forced the piston to eject the packaged sphere from the container. The piston's travel was restrained by the wire rope cable assembly. (See fig. 27.) In the extended position, the bellows were approximately 19.1 inches long.

The disconnect mechanism is shown in figure 27. The main basic parts of the disconnect mechanism were made of stainless steel and the disconnect switch was made by nylon and copper. The disconnect mechanism had six basic parts which are as follows:

(1) The disconnect body by which the disconnect mechanism is attached to the bellows piston,

(2) A sliding sleeve that retains the detent balls and one of the steel balls on the wire rope cable assembly,

(3) Two rows of detent balls that were used to lock and unlock the various parts of the mechanism in their functional positions,

(4) A valve-stem extension which slides within the sleeve. The valve stem on the package sphere is attached to this extension. The nitrogen flows through the valve stem and extension into the sphere,

(5) A disconnect spring retained in a partially compressed state between disconnect body and the valve-stem extension, and

(6) A wire rope cable assembly which connects the inflation bottle and the disconnect mechanism. This assembly limits the travel of the bellows piston. One of the steel balls functions as a ball cock at the inlet end of the valve-stem extension. The cable is located within the bellows.

L
1
2
5
1

Four steps in the operation of the disconnect mechanism are shown in figure 28. Position number 1 shows the relationship of the disconnect parts prior to firing of the squibs. The two rows of detent balls are holding the valve-stem extension against the force of the valve spring.

Position number 2 shows the disconnect mechanism at the limit of travel of the wire rope. The body of the disconnect that is fastened to the bellows piston continues its travel by the continuing travel of the piston. This additional travel compresses the valve spring and allows the first row of detent balls to aline themselves with a machined recess in the disconnect body and thereby unlock the valve-stem extension from the sleeve. The valve spring is now free to relieve part of its compression and draws the valve-stem extension forward and opens the ball cock inlet port. The forward movement of the valve-stem extension is stopped by the second row of detent balls and by the lip on the forward end of the sleeve (position number 3).

The disconnect mechanism remains in position number 3 until the sphere is completely inflated. Practically all of the nitrogen is required to inflate the sphere; and a decrease in nitrogen pressure in the bellows results. When the internal pressure of the bellows drops to about 0.1 pound per square inch, the sphere is completely inflated and has an internal pressure of approximately 0.1 pound per square inch. The valve spring then overcomes the force exerted by the bellows piston that is holding the disconnect body in its most forward position and returns the disconnect body to its starting position. During the rearward movement of the disconnect body, the second row of detent balls that are locking the valve-stem extension are released into a machined recess in the disconnect body and thereby permanently frees the valve-stem extension (position number 4).

The valve spring, now reacts to release one of its restricting parts, pulls the valve-stem extension from the disconnect body, and simultaneously imparts a separation energy to the satellite. After separation of the inflated sphere from the disconnect mechanism, the internal pressure in the sphere equalizes with the outside pressure through the open valve stem.

Jupiter-C Package

The 12-foot-diameter inflatable sphere and the inflation, ejection, and disconnect systems were designed for use as a Jupiter-C payload. The inflatable sphere was constructed from the three-ply laminate. The launching vehicle was a five-stage Jupiter-C consisting of a modified Redstone, first-stage, and a high-speed assembly containing four stages. The high-speed assembly combined the second, third, and fourth stages as well as the payload which contained the fifth-stage kick motor.

The fourth-stage motor and the payload assembly are shown in figure 29. The payload assembly was contained in a cylindrical shell 7 inches in diameter and approximately 55 inches long. The payload assembly separates from the fourth-stage motor after burnout. The kick motor, fifth stage, is located in the nose of the payload with the nozzle facing forward. When the kick motor is fired on signal from the timer, the nose tip is blown off, and the nozzle is exposed. The kick motor is fired at first apogee and since the payload assembly has a fixed orientation in space because of spin stabilization, the direction of thrust at apogee is such as to increase the payload velocity. The increase in thrust results in a new orbit with a much higher perigee. A signal from the timer activates the squibs and starts the inflation sequence. L 1 2 5 1

Juno II Package

The 12-foot-diameter inflatable sphere fabricated from the three-ply laminate and the inflation, ejection, and disconnect systems that were used as the Juno II payload were similar to those used as the Jupiter-C payload. The launching vehicle consisted of a modified Jupiter first stage and a two-stage high-speed cluster. The payload was attached to the forward end of the third-stage adapter.

The third-stage motor assembly and the payload assembly are shown in figure 30. The payload was contained in a cylindrical shell 7 inches in diameter and approximately 24 inches long. At burnout of the third stage, the third-stage assembly and the payload were expected to be in orbit. The third-stage timer was to be used to initiate the sequence of ejection, inflation, and release of the sphere.

Scout Payload

The 12-foot-diameter inflatable sphere payload (fig. 23) for the Scout launching vehicle was similar to the ones developed for the Jupiter-C and Juno II launching vehicles. The major differences were a four-ply laminate sphere, the diameter of the payload container, and

the method of initiating the sequence of events: ejection, inflation, and separation.

Because of the addition of the radio tracking beacon to the sphere, the diameter of the payload container was increased to 8.5 inches. This increase required a redesign of the ejection bellows and its restraining wire rope cable to compensate for the larger diameter but retaining all other characteristics.

The sequence of events in the operation of the Scout payload was initiated when the chamber pressure of the fourth-stage rocket motor dropped to a predetermined value. A pressure switch on the thrust face of the fourth stage fired a series of pyrotechnics that activated the valve on the inflation bottle.

L
1
2
5
1

APPENDIX D

TEMPERATURE LIMITS ON THIN-WALL SPHERICAL SATELLITE

The temperature limits on thin-wall spherical satellites were calculated for orbital positions where the maximum and minimum equilibrium temperatures would be obtained. The temperature was assumed to be uniform through the skin and the conductive transfer of heat flow from the hotter to the colder regions of the satellite skin was assumed to be negligible because of the skin thickness.

The maximum temperature on the satellite occurs when the satellite is directly between the sun and the earth. In this position, the satellite receives direct solar radiation, solar radiation diffusely reflected from the earth's surface, and direct earth-emitted radiation. The hottest spot on the satellite will be the unit of area that directly faces the sun. The expression for the maximum equilibrium temperature (ref. 23) is

$$T_{l_{max}}^4 = \frac{C_S\alpha_S + \frac{1}{4}\frac{\epsilon_i}{\epsilon_o} C_S\alpha_S\left(1 + 2\left\{a + \left(\frac{1-a}{4}\right)\left(\frac{\alpha_E}{\alpha_S}\right)\left[1 - (1-k^2)^{1/2}\right]\right\}\right)}{\sigma(\epsilon_i + \epsilon_o)}$$

An expression is also needed for the minimum equilibrium skin temperature while the satellite is directly between the earth and the sun. The minimum temperature will be located about 90° from the point of maximum skin temperature. Because of the high angle of incidence, the direct contributions of flux are assumed to be negligible and the only contribution of flux is that radiated from the inside surface of the satellite. The conservative expression derived for the minimum equilibrium skin temperature while the satellite is directly between the earth and the sun is

$$T_{l_{min}}^4 = \frac{\frac{1}{4}\frac{\epsilon_i}{\epsilon_o} C_S\alpha_S\left(1 + 2\left\{a + \left(\frac{1-a}{4}\right)\left(\frac{\alpha_E}{\alpha_S}\right)\left[1 - (1-k^2)^{1/2}\right]\right\}\right)}{\sigma(\epsilon_i + \epsilon_o)}$$

The temperature of the coldest spot on the satellite will be obtained when the satellite is in the earth's shadow and is receiving only the earth's emitted radiation. The minimum temperature will be experienced on the side of the satellite opposite the earth where only

L 1 2 5 1

the radiation transmitted by the inside of the satellite is received. The minimum equilibrium temperature (ref. 23) is

$$T_{2_{min}}^4 = \frac{\frac{1}{4}\frac{\epsilon_i}{\epsilon_o} C_S \alpha_E \left(\frac{1 - a}{2}\right)\left[1 - \left(1 - k^2\right)^{1/2}\right]}{\sigma(\epsilon_i + \epsilon_o)}$$

The maximum equilibrium temperature for the satellite while in the earth's shadow will be that portion of the satellite's skin facing the earth that receives the maximum direct earth radiation per unit area. Here, thermal balance will be obtained when the reception from the earth plus reception from the inside skin equals the radiation from both sides of the satellite skin closest to the earth. The expression for the maximum temperature (from ref. 24) while in the earth's shadow is

$$T_{2_{max}}^4 = \frac{C_S \alpha_E \left(\frac{1 - a}{4}\right)\left\{\frac{1}{2}\frac{\epsilon_i}{\epsilon_o}\left[1 - \left(1 - k^2\right)^{1/2}\right] + k^2\right\}}{\sigma(\epsilon_i + \epsilon_o)}$$

In order to decrease the maximum skin temperature while the satellite is in the sunlight, the average absorbtivity and emissivity of the outside skin may be changed. This change may be accomplished by uniformly coating a percentage of the total outside surface area. The effective absorbtivity and emissivity may then be expressed as

$$\alpha_S = \left(\alpha_{S,p} - \alpha_{S,u}\right)\frac{A_c}{A_T} + \alpha_{S,u}$$

$$\epsilon_o = \left(\epsilon_{o,p} - \epsilon_{o,u}\right)\frac{A_c}{A_T} + \epsilon_{o,u}$$

REFERENCES

1. Van Allen, James A., ed.: Scientific Uses of Earth Satellites. Univ. of Michigan Press (Ann Arbor), c.1956.

2. Sterne, T. E., and Schilling, G. F.: Some Preliminary Values of Upper Atmosphere Density From Observations of USSR Satellites. Special Report No. 3, Smithsonian Institution Astrophysical Observatory, Nov. 15, 1957.

3. Sterne, T. E., Folkart, B. M., and Schilling, G. F.: An Interim Model Atmosphere Fitted to Preliminary Densities Inferred From USSR Satellites. Special Report No. 7, Smithsonian Institution Astrophysical Observatory, Dec. 31, 1957.

4. Harris, I., and Jastrow, R.: Upper Atmospheric Densities From Minitrack Observations on Sputnik I. Science, vol. 127, no. 3296, Feb. 28, 1958, pp. 471-472.

5. Jacchia, L. G.: The Secular Perturbations and the Orbital Acceleration of Satellite 1958 Beta Two. Special Report No. 12, Smithsonian Institution Astrophysical Observatory, Apr. 30, 1958, pp. 30-33.

6. Kallmann, H. K., and Juncosa, M. L.: A Preliminary Model Atmosphere Based on Rocket and Satellite Data. U.S. Air Force Project RAND Res. Memo. RM-2286 (ASTIA Doc. No. AD 207752), The RAND Corp., Oct. 30, 1958.

7. Harris, I., and Jastrow, R.: An Interim Atmosphere Derived From Rocket and Satellite Data. A.4, Nat. Res. Council, Nat. Acad. Sci., 1958.

8. Sterne, Theodore E.: The Density of the Upper Atmosphere. Special Report No. 11, Smithsonian Institution Astrophysical Observatory, Mar. 31, 1958, pp. 18-22.

9. Groves, G. V.: Effect of the Earth's Equatorial Bulge on the Life-Time of Artificial Satellites and Its Use in Determining Atmospheric Scale-Heights. Nature (Letters to the Editor), vol. 181, no. 4615, Apr. 12, 1958, p. 1055.

10. DeBey, L. G., Berning, W. W., Reuyl, D., and Cobb, H. M.: Scientific Objectives and Observing Methods for a Minimum Artificial Earth Satellite. Rep. No. 956, Ballistic Res. Labs., Aberdeen Proving Ground, Oct. 1955. (Available from ASTIA as Doc. No. AD 78570.)

11. Anon.: Mylar - Physical, Electrical, and Chemical Properties. Tech. Rep. TR-1, E. I. Du Pont de Nemours, Co., Inc., 1955.

12. Anon.: The Aluminum Data Book. Reynolds Metal Co. (Richmond, Va.), 1958.

13. Roark, Raymond J.: Formulas for Stress and Strain. Second ed., McGraw-Hill Book Co., Inc., 1943.

14. Kehlet, Alan B., and Patterson, Herbert G.: Free-Flight Test of a Technique for Inflating an NASA 12-Foot-Diameter Sphere at High Altitudes. NASA MEMO 2-5-59L, 1959.

15. Rose, James T., and Smith, R. Donald: A Radar Test Target System. NASA TN D-164, 1960.

16. Petersen, N. V.: Lifetimes of Satellites in Near-Circular and Elliptic Orbits. Jet Propulsion, vol. 26, no. 5, May 1956, pp. 341-351, 368.

17. Minzner, R. A., Champion, K. S. W., and Pond, H. L.: The ARDC Model Atmosphere, 1959. Air Force Surveys in Geophysics No. 115 (AFCRC-TR-59-267), Air Force Cambridge Res. Center, Aug. 1959.

18. Whipple, Fred L., and Hynek, J. Allen: Optical and Visual Tracking of Artificial Satellites. Proc. VIIIth Int. Astronautical Congress, Springer-Verlag (Wien), 1958, pp. 429-435.

19. Tousey, R., Koomen, M. J., and Gullege, I. S.: Stellar Magnitude of Vanguard Satellites and of the Vanguard Third Stage Rocket Casing. C.10, Nat. Res. Council, Nat. Acad. Sci., 1958.

20. Russell, Henry Norris: On the Albedo of the Planets and Their Satellites. The Astrophysical Jour., vol. XLIII, no. 3, Apr. 1916, pp. 173-196.

21. Tousey, R.: The Visibility of an Earth Satellite. Astronautica Acta, Vol. II, Fasc. 2, 1956, pp. 101-112.

22. Seely, Fred B.: Resistance of Materials. Second ed., John Wiley & Sons, Inc., c.1935.

23. Wood, George P., and Carter, Arlen F.: Predicted Characteristics of an Inflatable Aluminized-Plastic Spherical Earth Satellite With Regard to Temperature, Visibility, Reflection of Radar Waves, and Protection From Ultraviolet Radiation. NASA TN D-115, 1959.

24. Cunningham, F. G.: Power Input to a Small Flat Plate From a Diffusely Radiating Sphere, With Application to Earth Satellites. NASA TN D-710, 1961. (Corrected copy.)

TABLE I.- MECHANICAL AND PHYSICAL PROPERTIES OF ALUMINUM AND MYLAR

Property	Aluminum	Mylar
Tensile strength, lb/sq in.	4,125	20,000
Modulus of elasticity, lb/sq in.	10.3×10^6	5.5×10^5
Poisson's ratio	0.33	Assumed to be 0
Density, gm/cc	2.70	1.39
Melting point, °C	660	250 - 255
Specific heat, cal/gm/°C	0.214 at 100°	0.315 at 25° 0.476 at 200°

L
1
2
5
1

TABLE II.- EMISSIVITY AND SOLAR ABSORPTIVITY VALUES

Material	Emissivity, ϵ	Absorptivity, α_s	α_s/ϵ
Aluminum foil	0.08	0.15	1.875
Mylar	.5		
White epoxy paint	.90	.33	.367

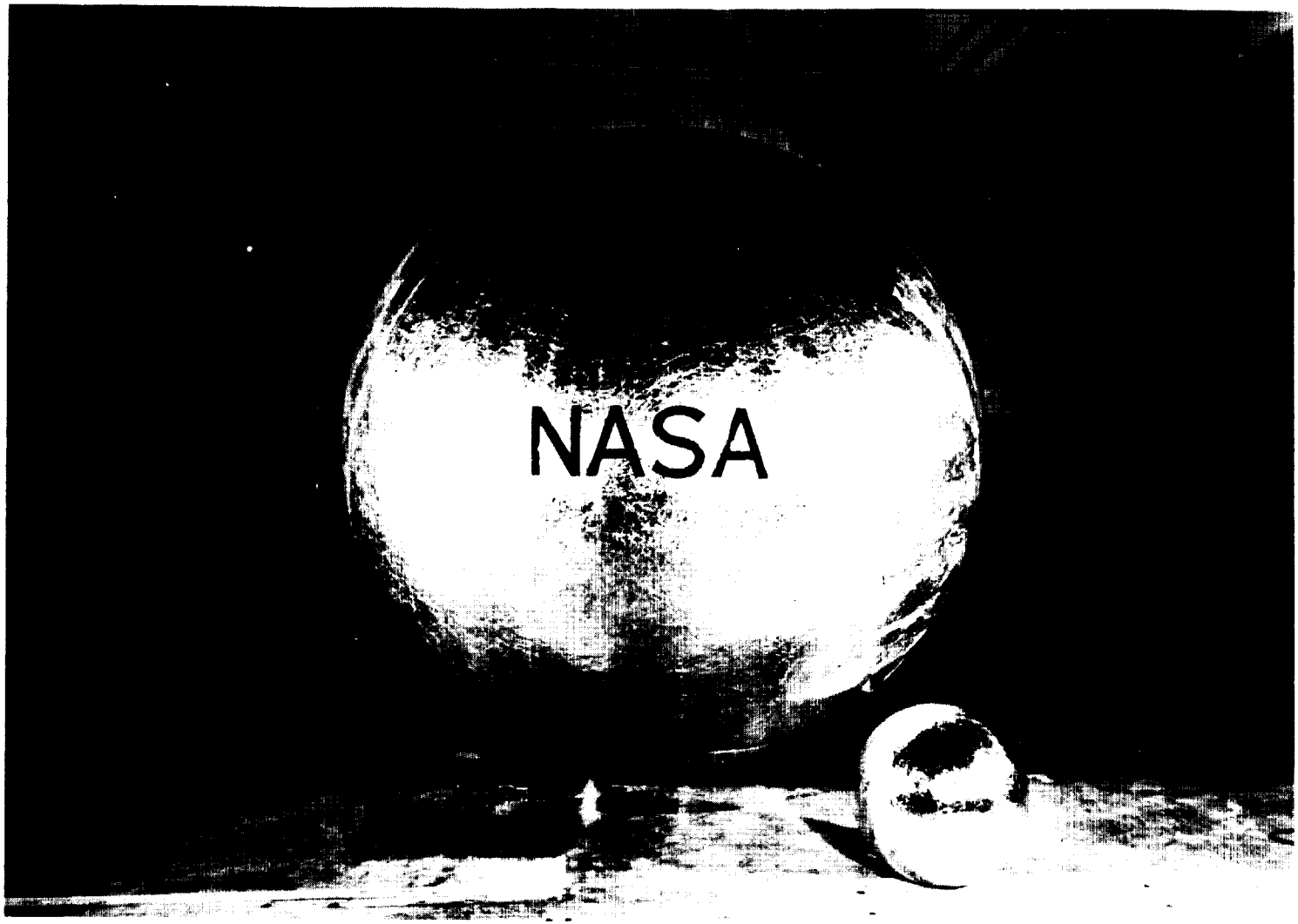

L-58-1076a

Figure 1.- Photograph of the inflated 30-inch- and 12-foot-diameter spheres.

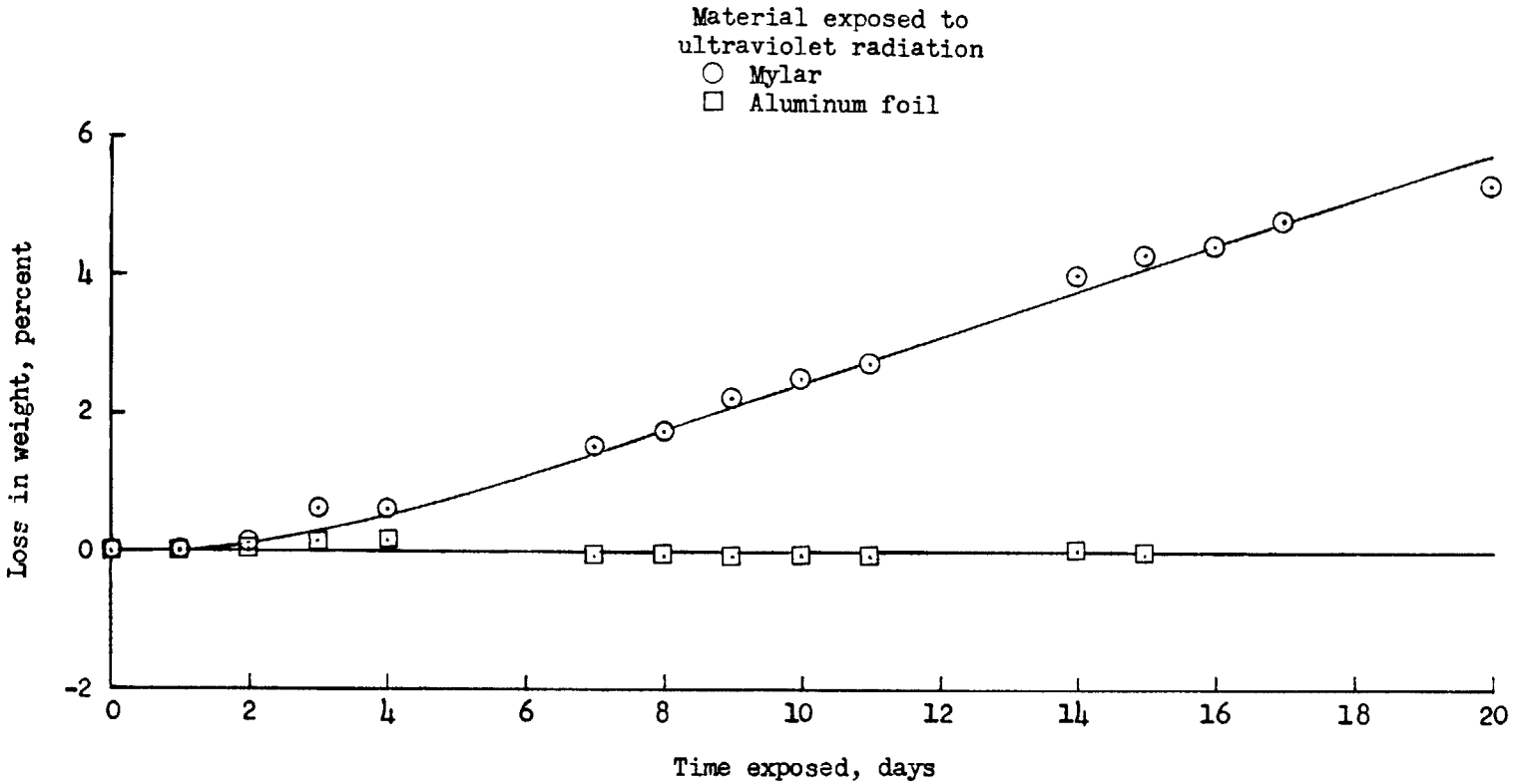

Figure 2.- Percent loss in weight of the 2-ply laminate (aluminum foil-Mylar) exposed to ultraviolet radiation (Mercury quartz arc lamp, Hanovia Chemical and Manufacturing Company, type 16000).

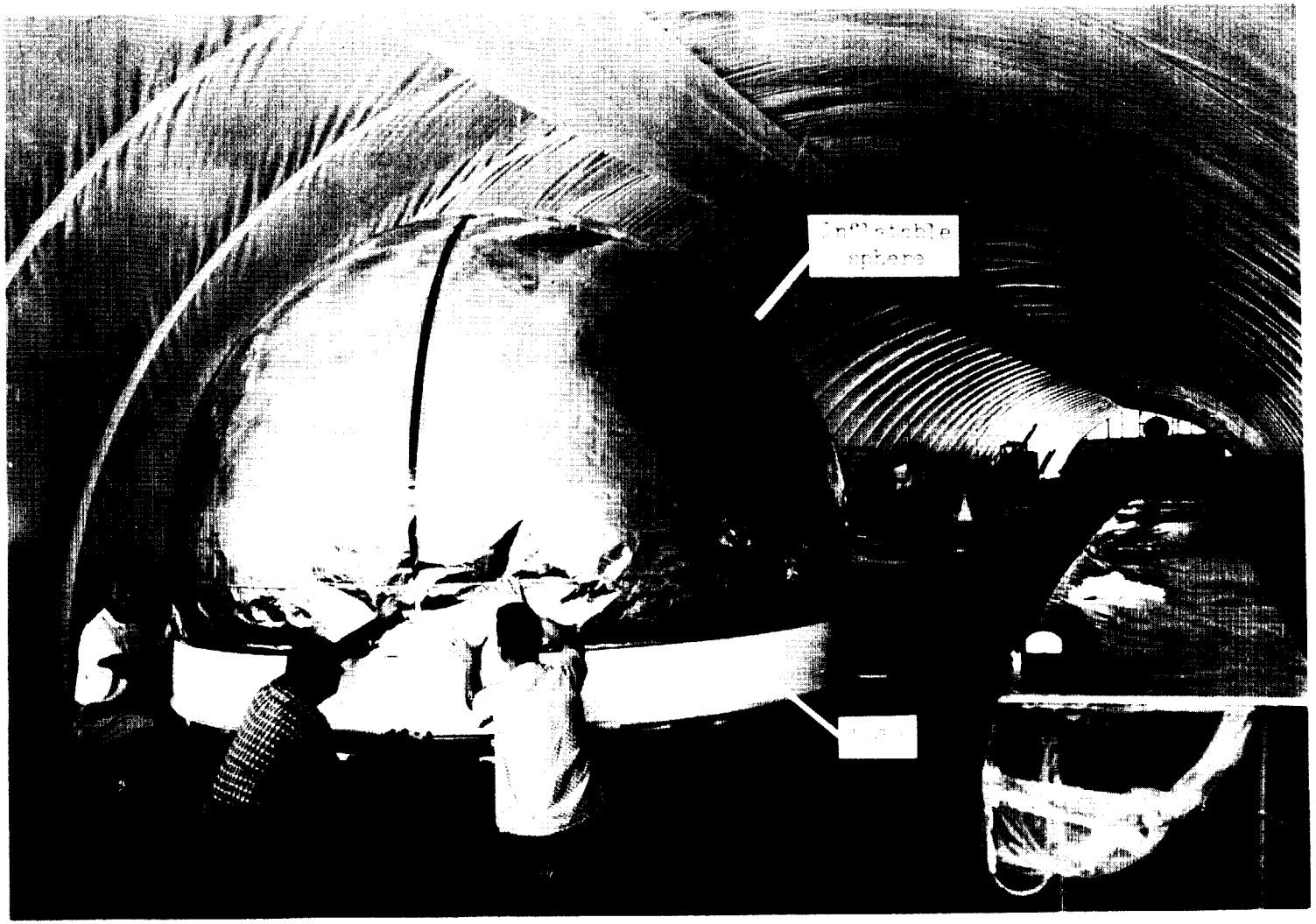

L-60-6008.1

Figure 3.- Removal of a 12-foot-diameter sphere from the hemispherical mold.

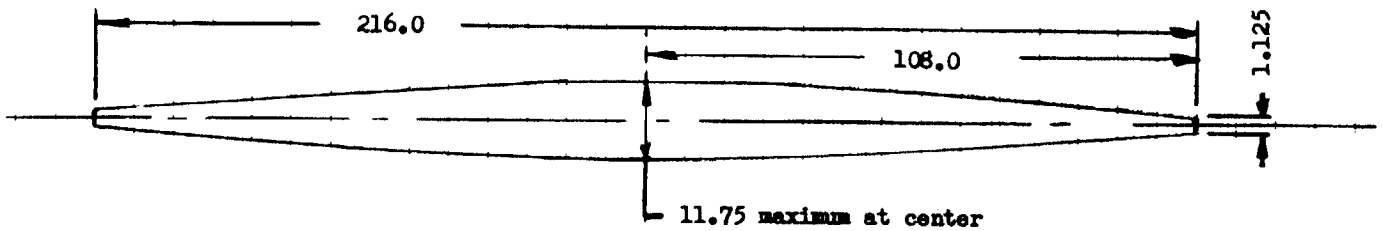

(a) Typical gore, 40 required.

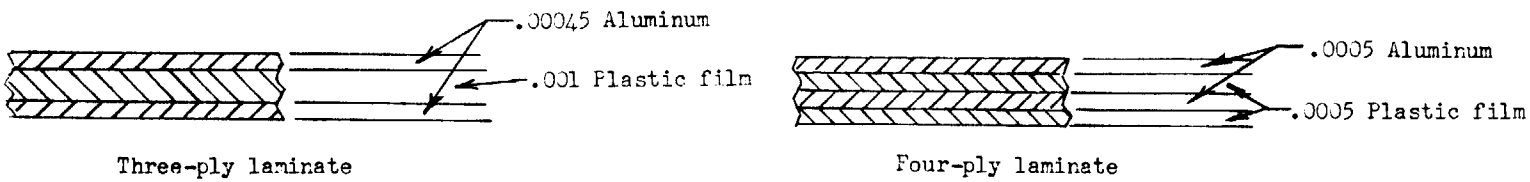

(b) Construction of aluminum-plastic film skin.

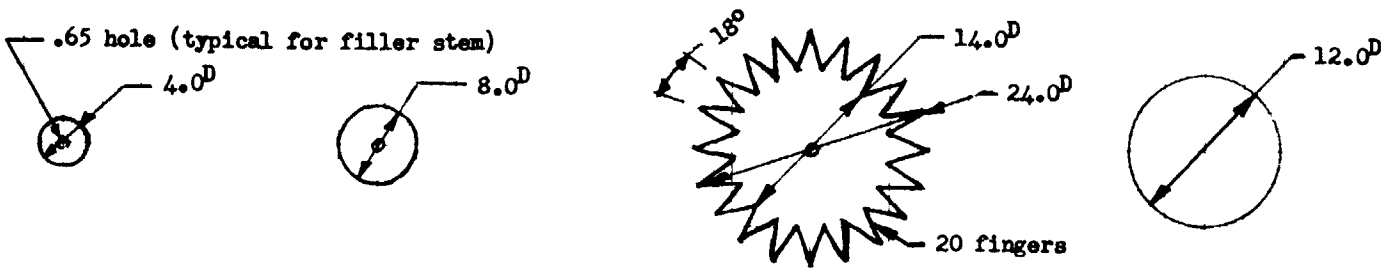

(c) Reinforcing patches at intersection of gores around base of filler stem. Material, Fairprene 5769.

(d) Reinforcing patch for end of sphere opposite filler stem. Material, silk.

Figure 4.- Construction and material details of the 12-foot-diameter inflatable sphere. (All dimensions are in inches.)

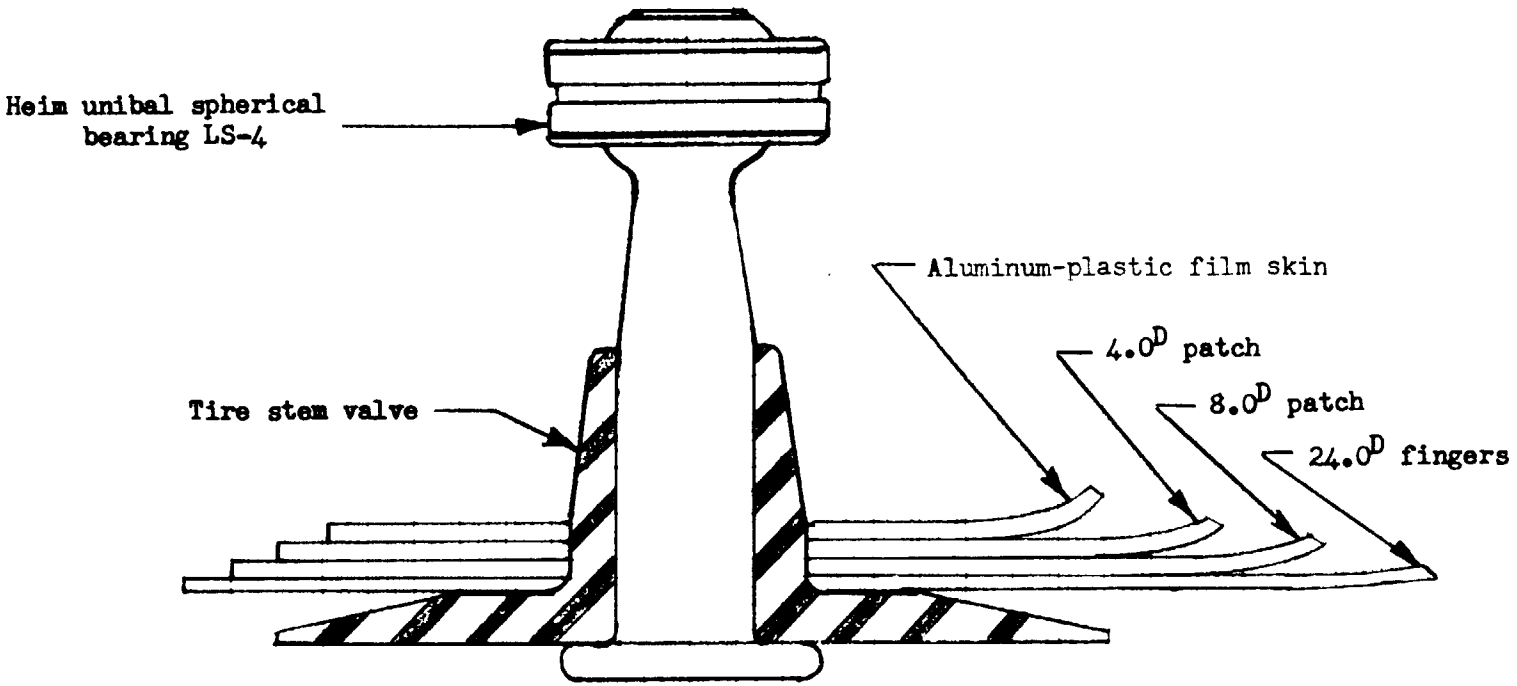

(e) Detail at intersection of gores showing reinforcement patches and filler stem.

Figure 4.- Concluded.

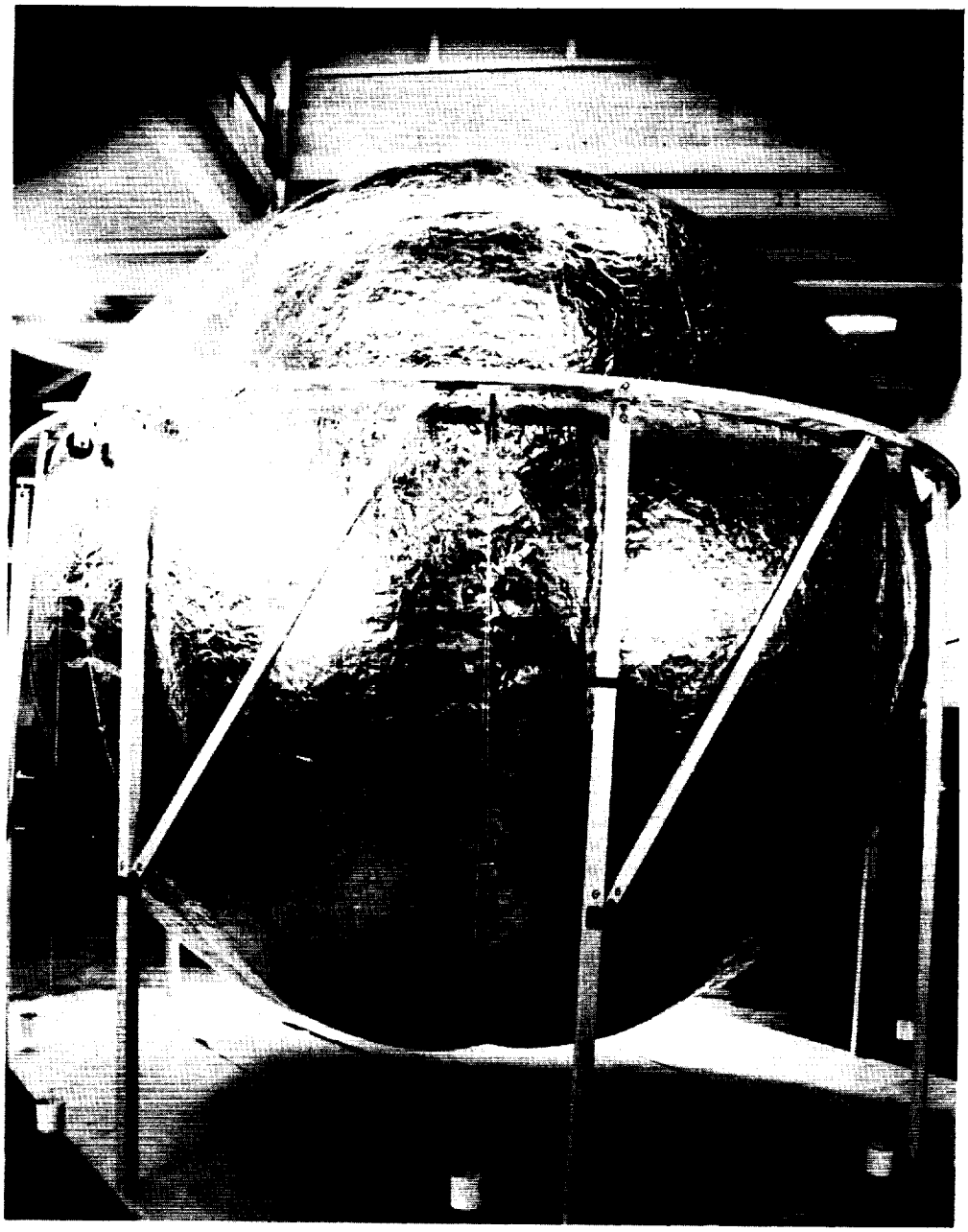

L-57-5467

Figure 5.- Photograph of the testing of a 12-foot-diameter inflatable sphere.

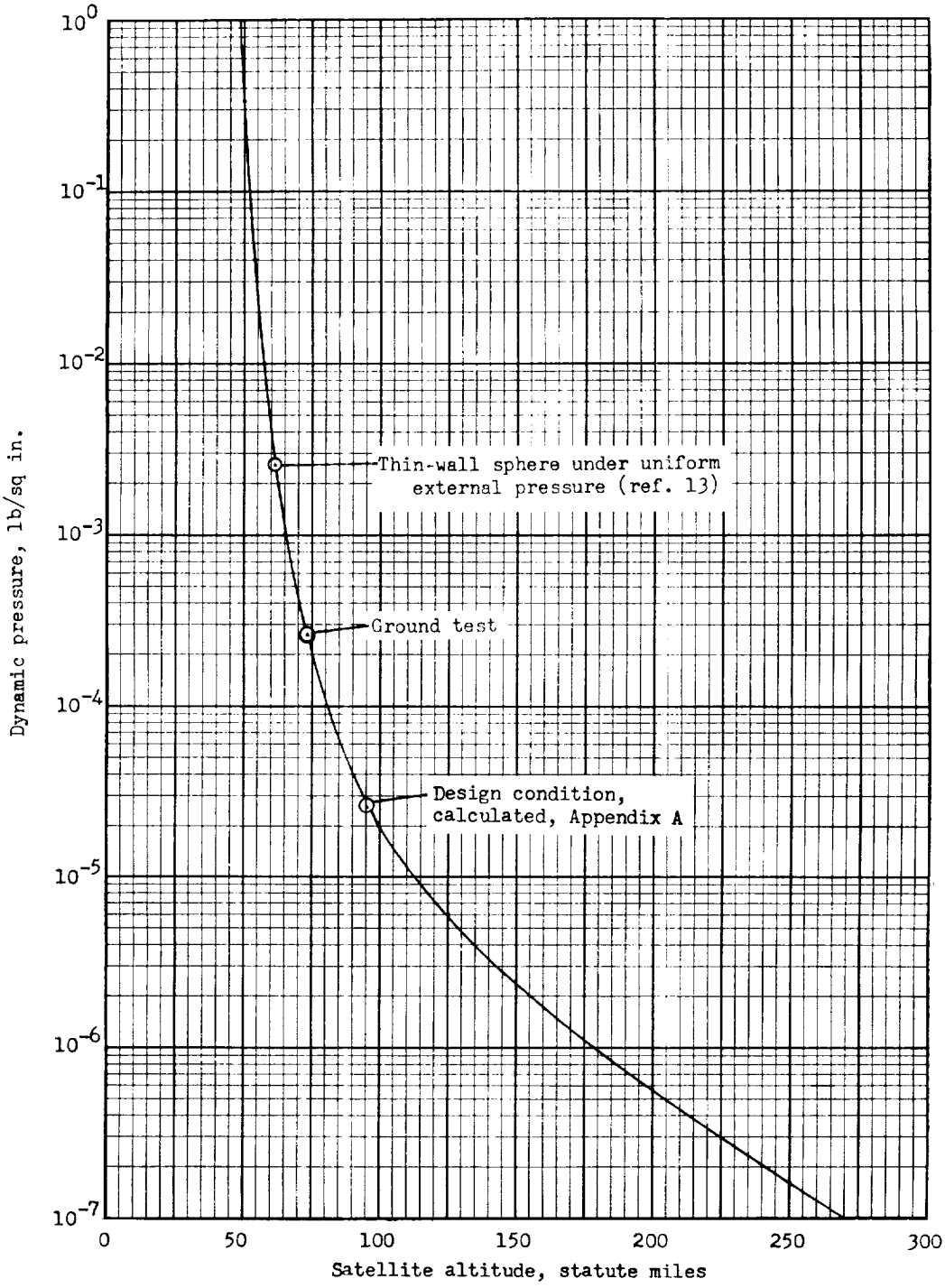

Figure 6.- Variation of dynamic pressure with satellite altitude for the 12-foot inflatable spheres.

L-59-2821

(a) Basic pleated pattern.

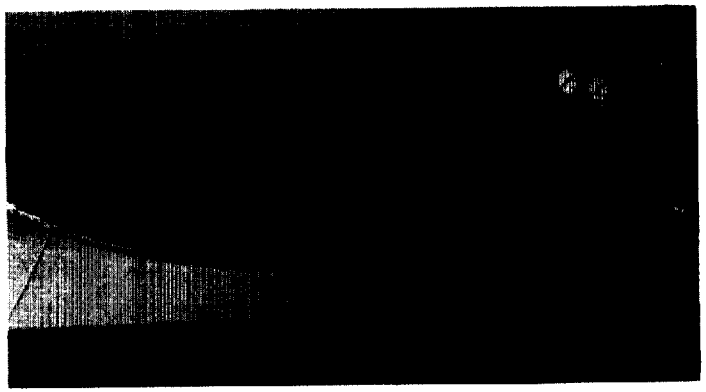

L-59-2822

(b) Flat shape after basic pattern.

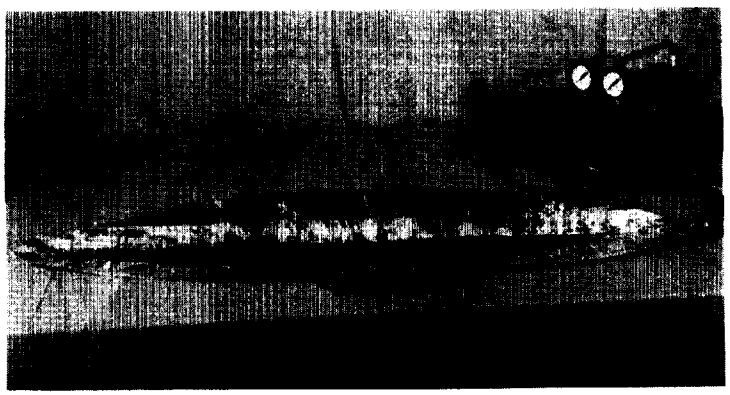

(c) Accordion fold. L-59-2823

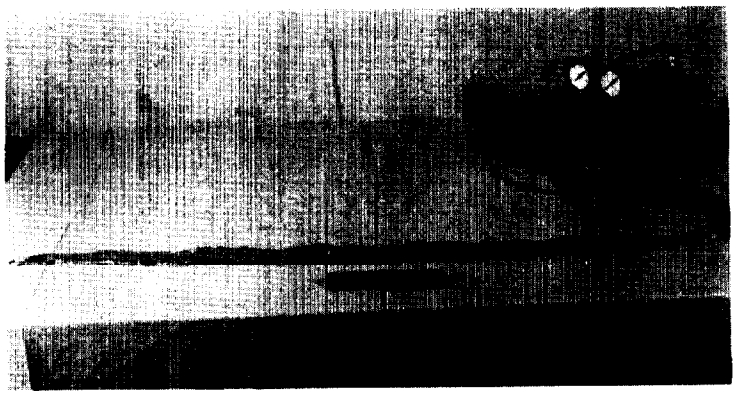

(d) Final flat streamer. L-59-2824

Figure 7.- Photographs of the general folding process of a 30-inch-diameter inflatable sphere.

(a) Annular package (30-inch sphere). L-59-2827

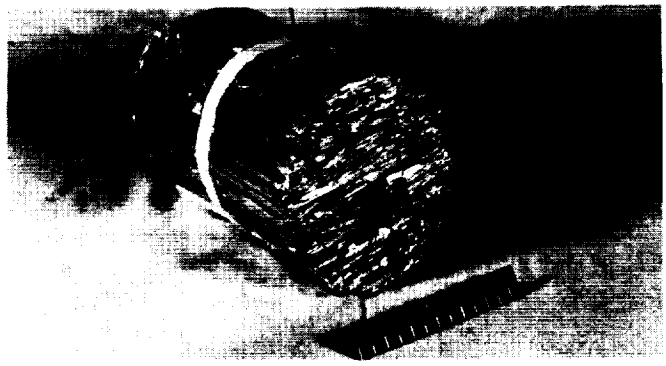

(b) Cylindrical package (12-foot sphere). L-59-2836

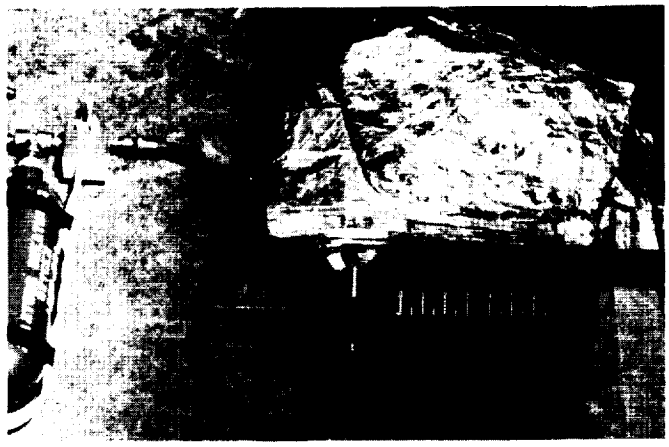

(c) Flat package (12-foot sphere). L-58-2329

Figure 8.- Photographs showing the inflatable spheres folded to fit various payload compartments.

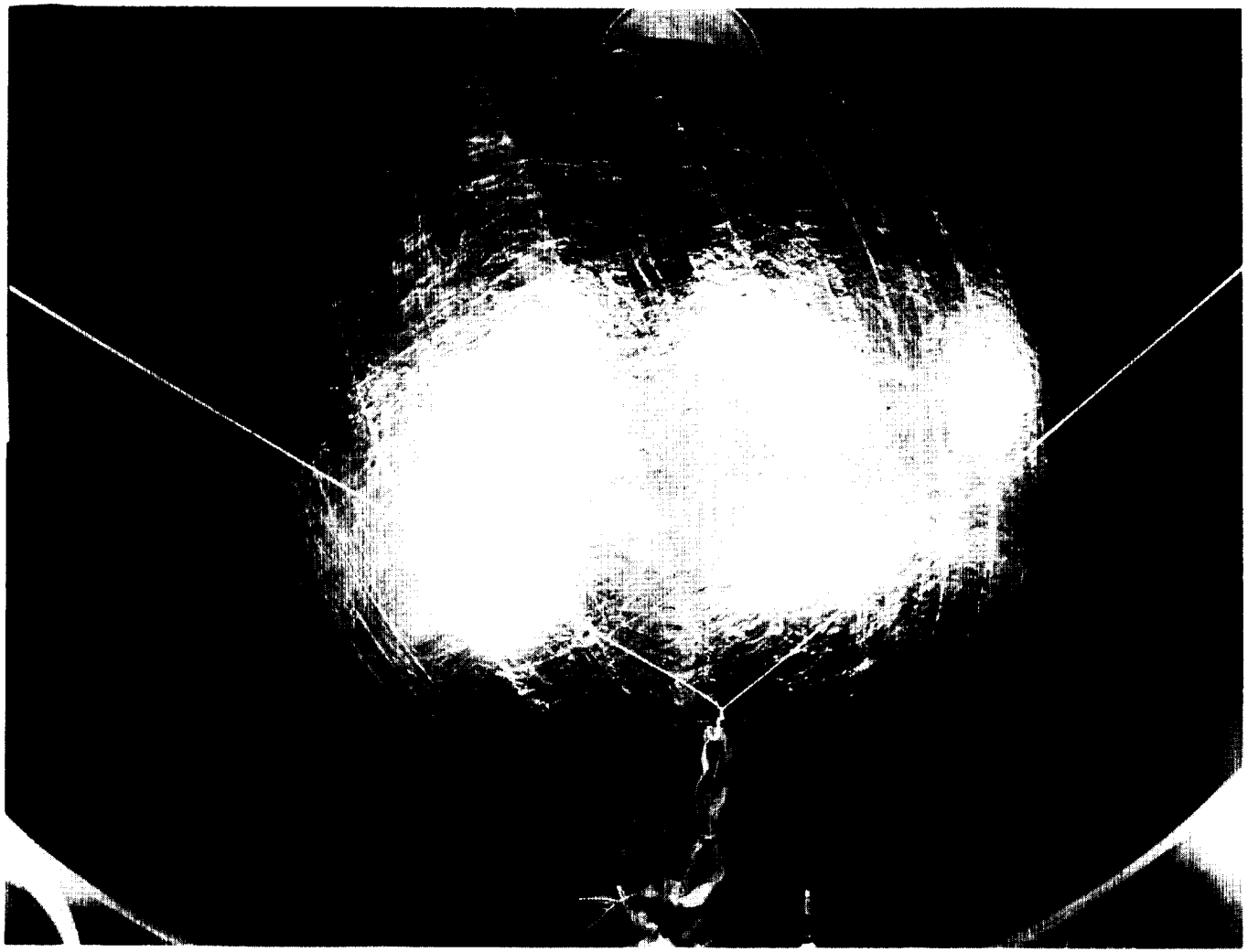

L-58-1317a

Figure 9.- Photograph of a 30-inch-diameter sphere after inflation in a vacuum tank.

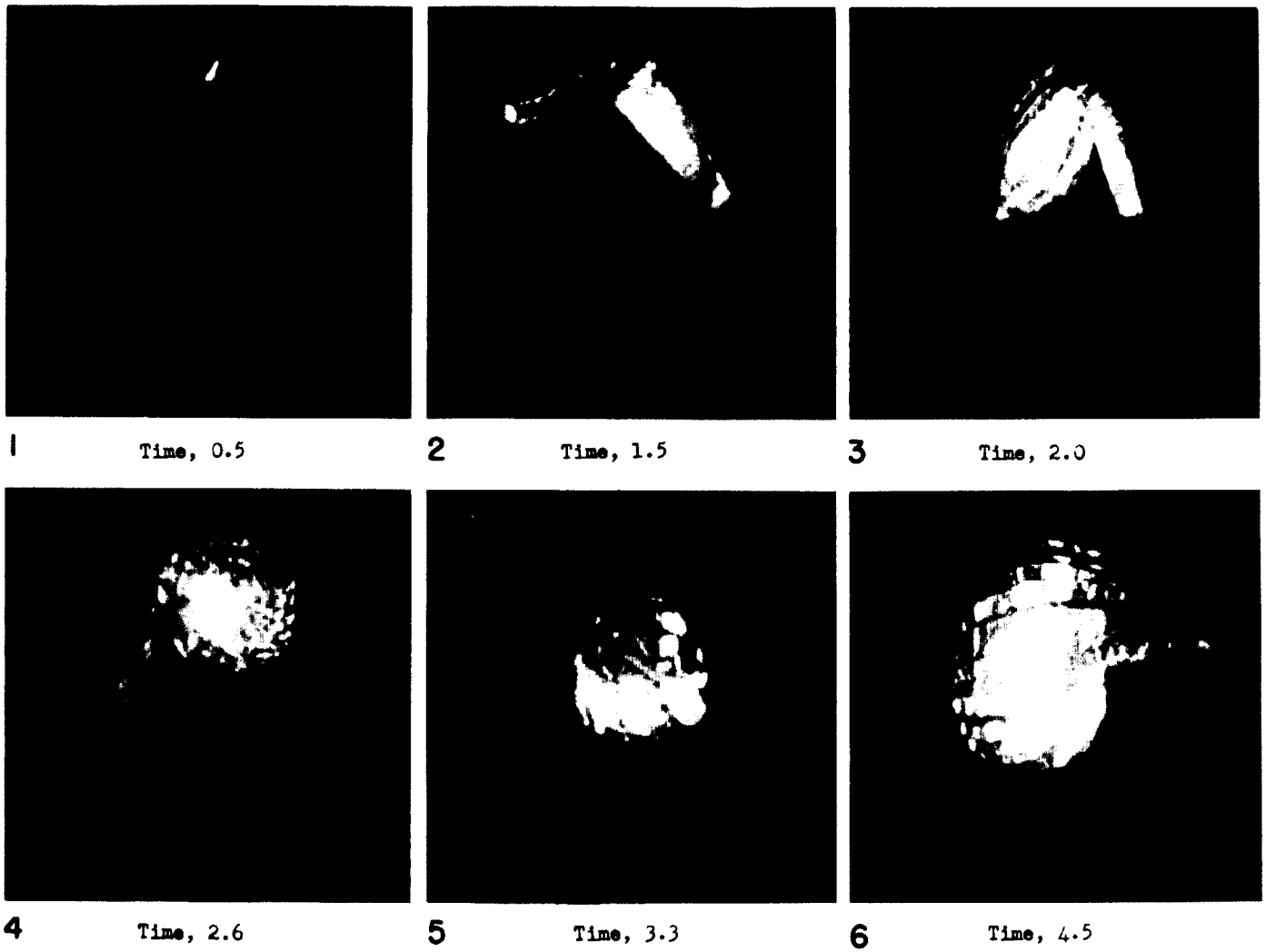

L-58-1543.1

Figure 10.- Photographs of a 12-foot-diameter sphere being inflated in a vacuum tank. (All times are seconds after activation of the inflation bottle.)

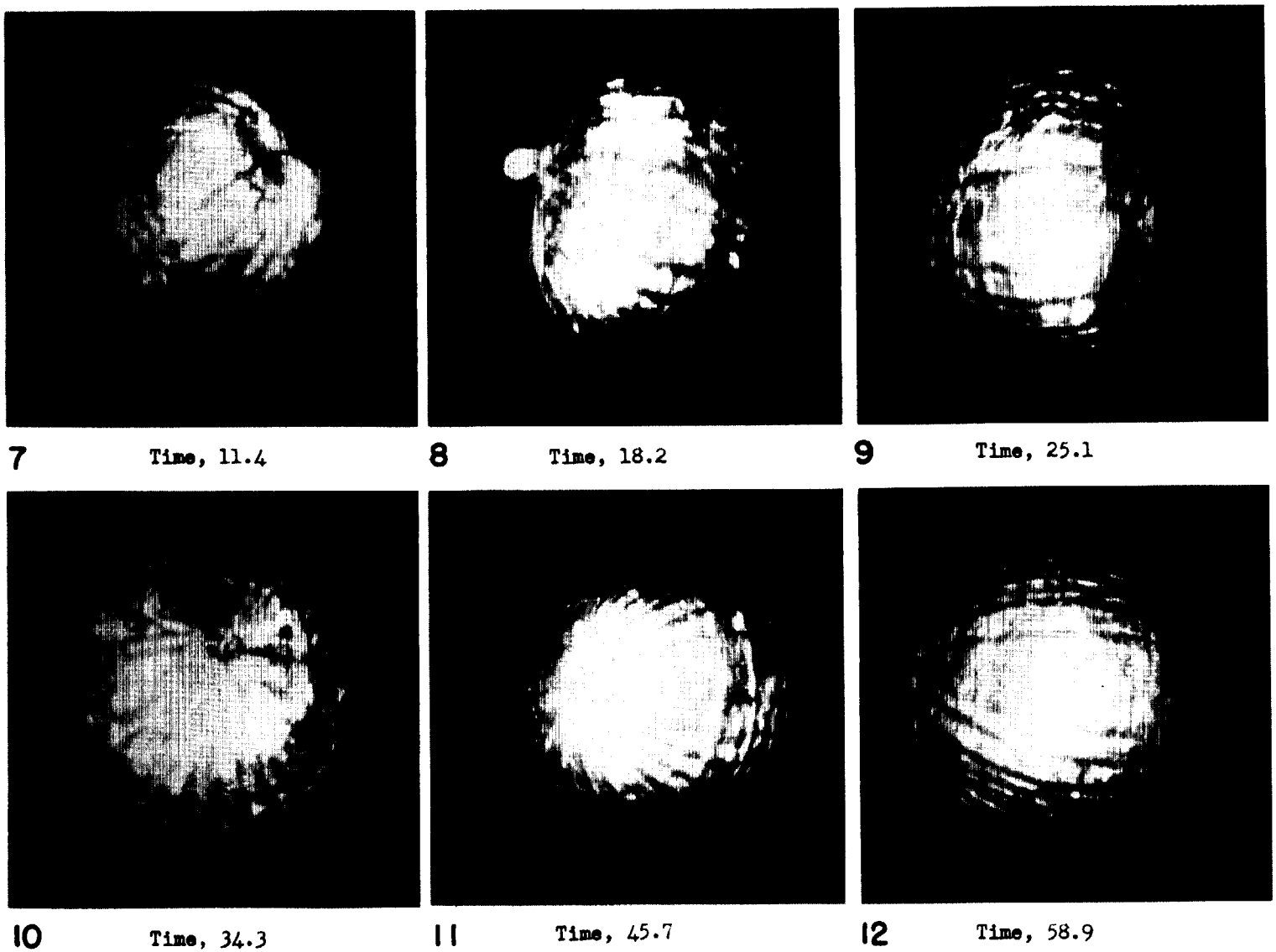

Figure 10.- Continued.

L-58-1544.1

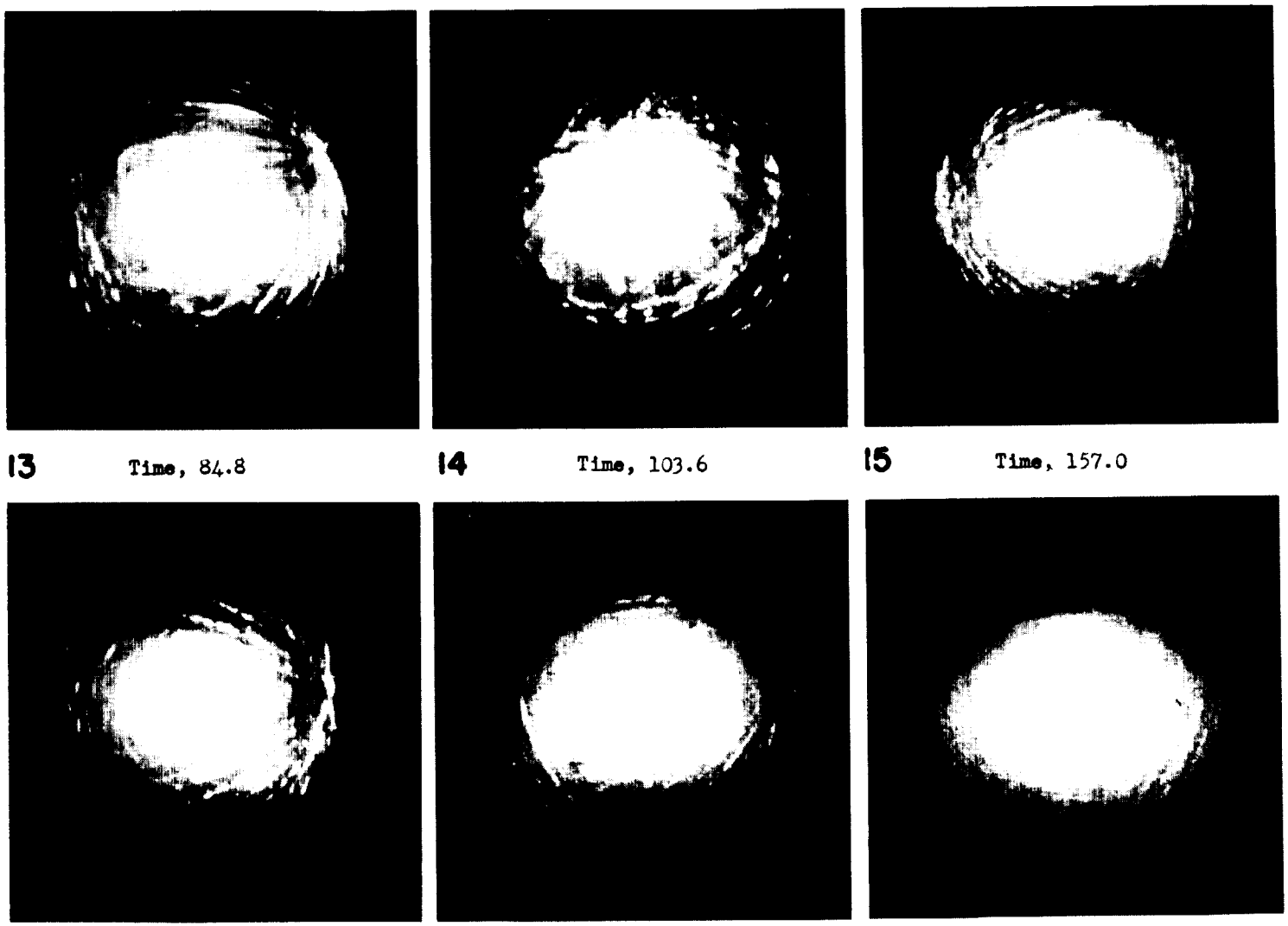

Figure 10.- Concluded.

L-58-1545.1

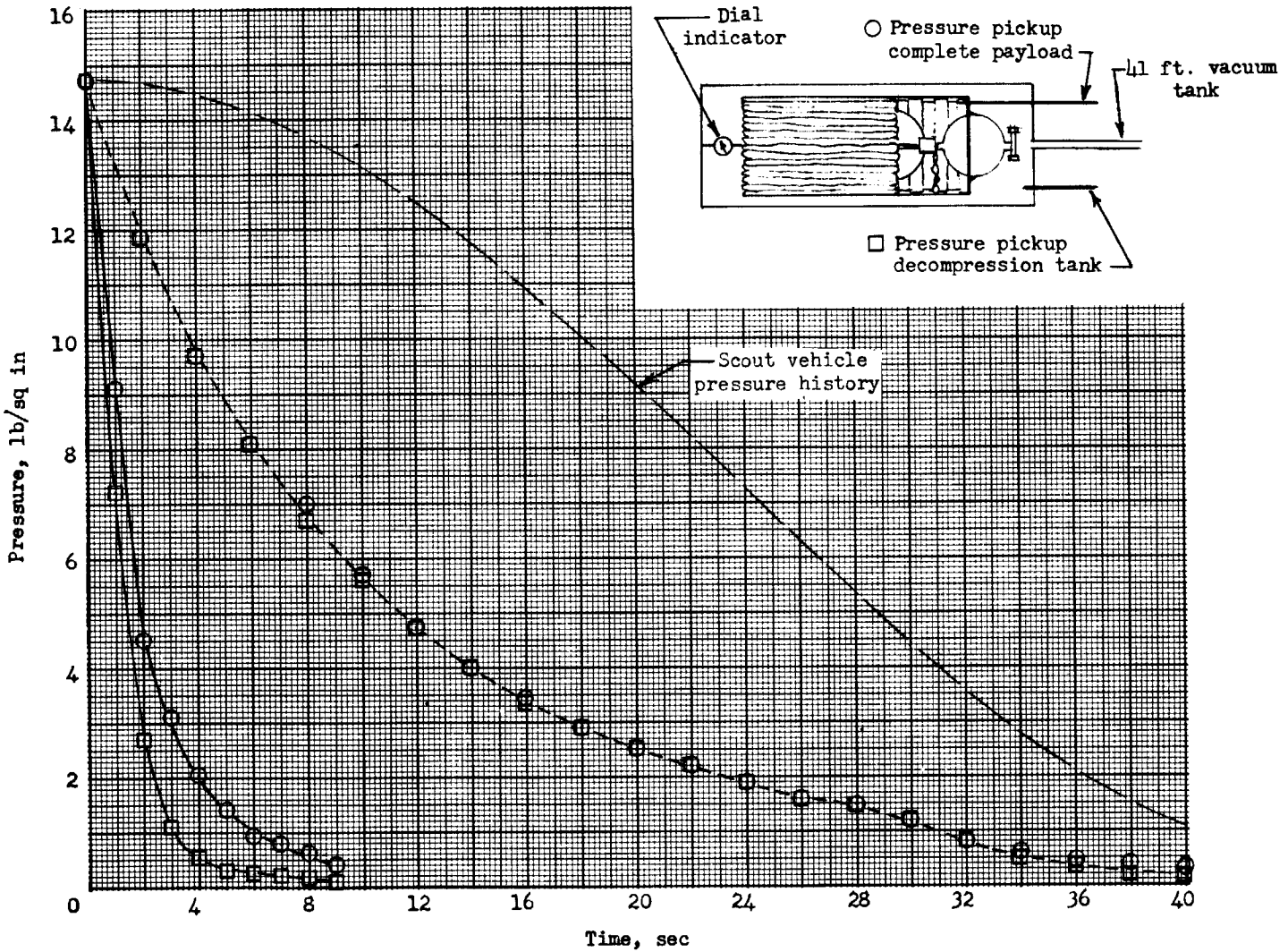

Figure 11.- Decompression tests of a 12-foot-diameter sphere payload package.

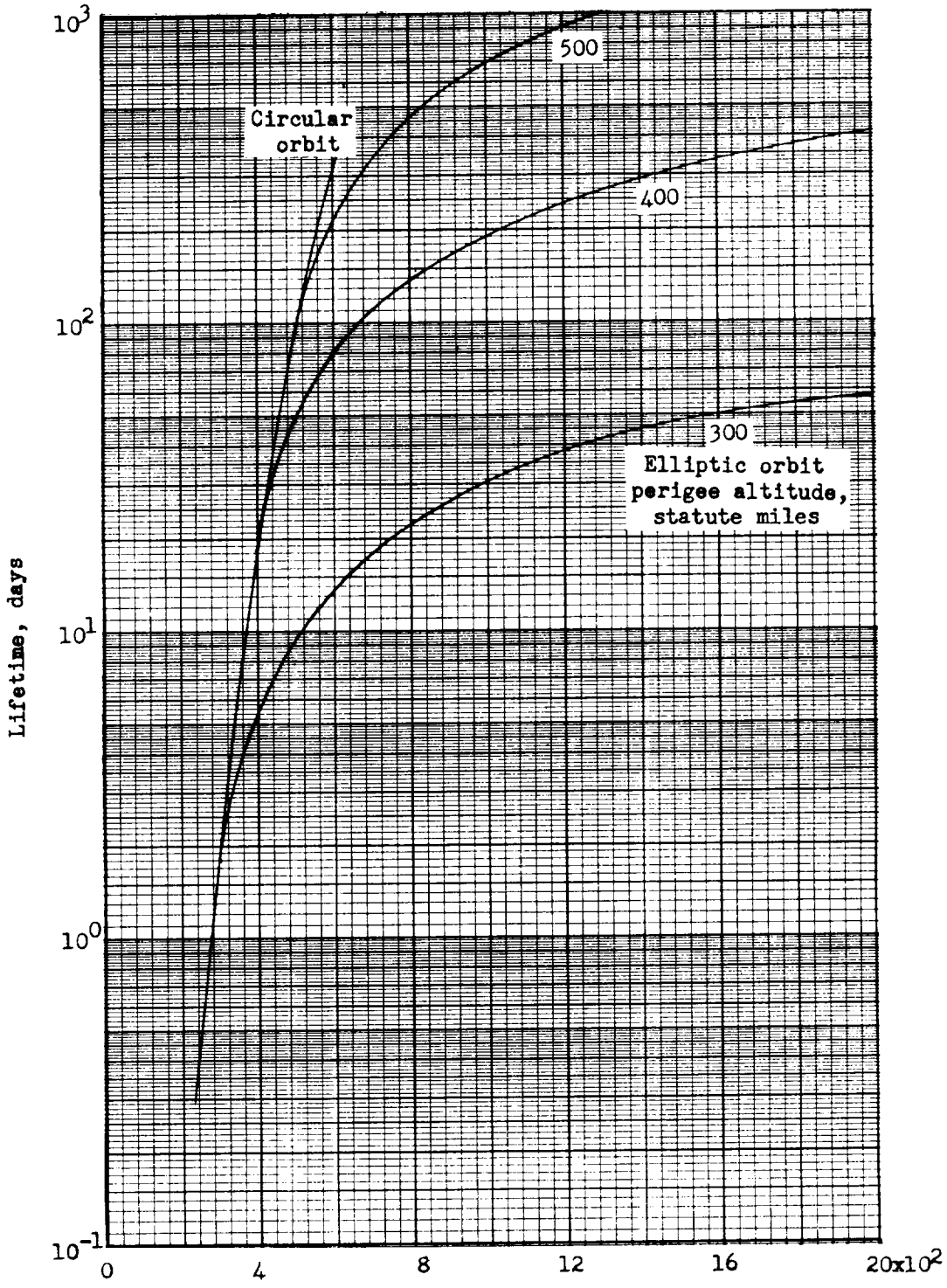

Figure 12.- Estimated lifetime of the 12-foot-diameter inflatable sphere. Weight, 15 pounds.

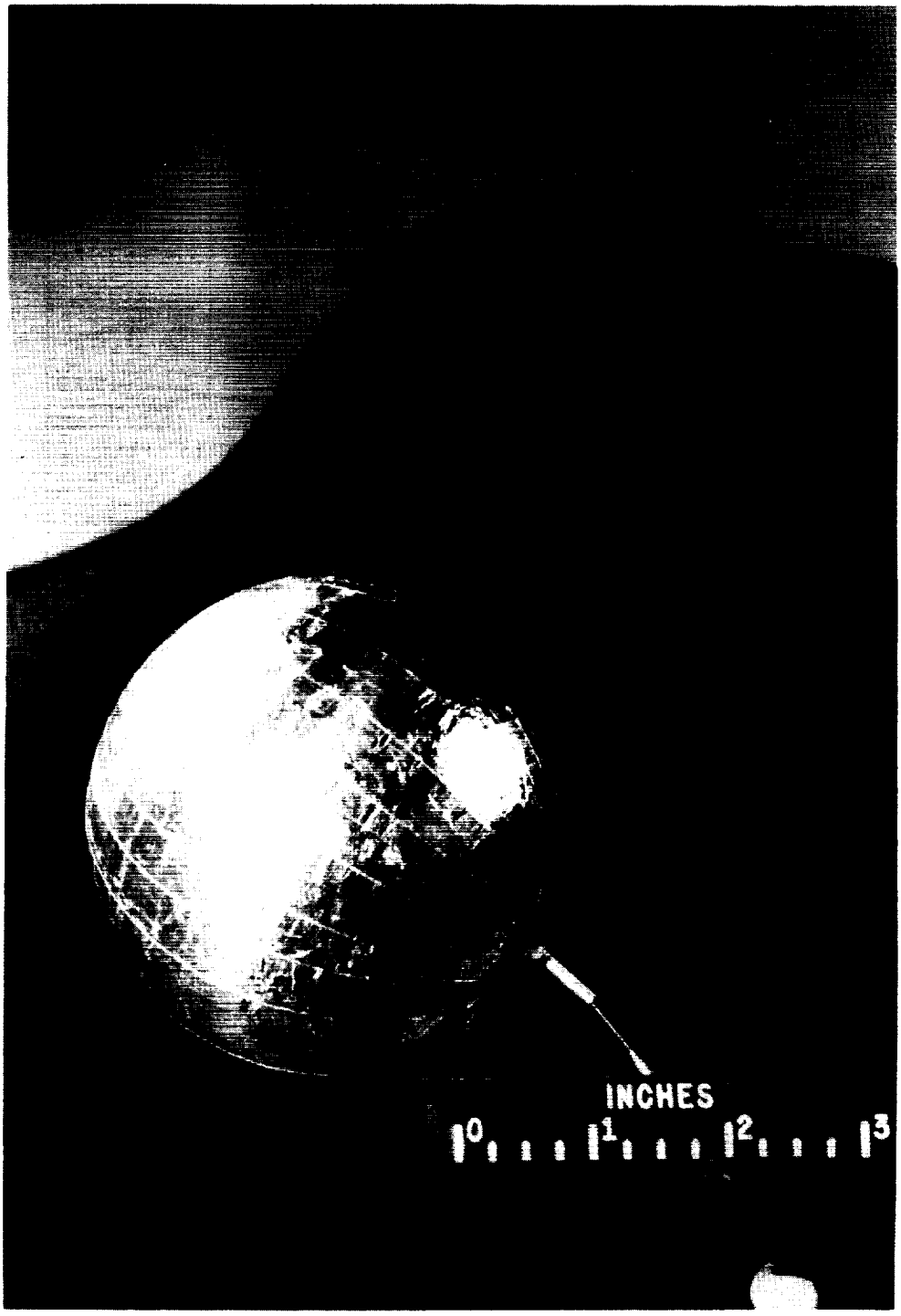

L-1251

L-57-875

Figure 13.- Photograph of a 4-inch-diameter inflatable sphere.

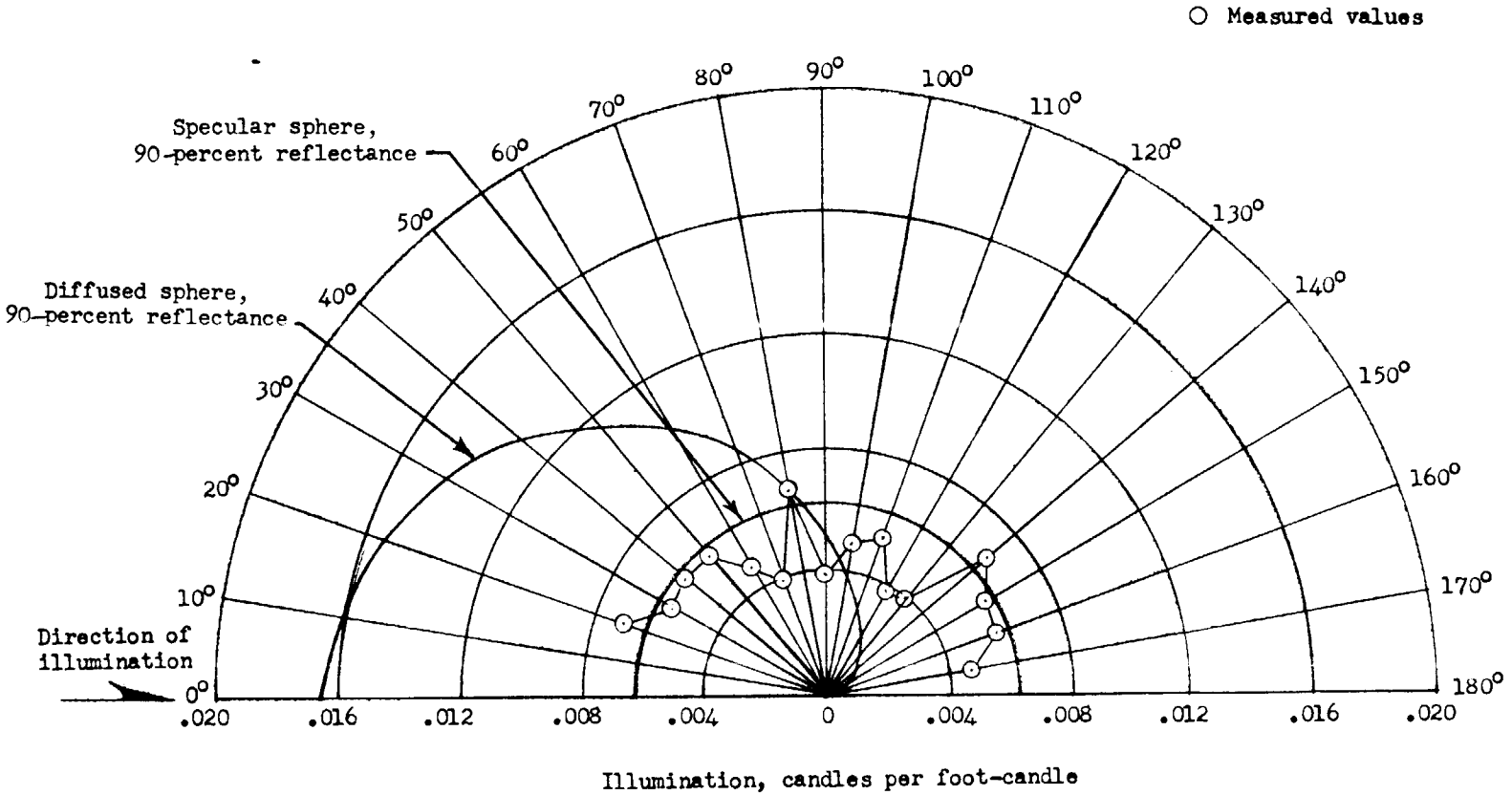

Figure 14.- Reflectance of a 4-inch-diameter inflatable sphere compared with calculated values of 90-percent specular and diffused spheres.

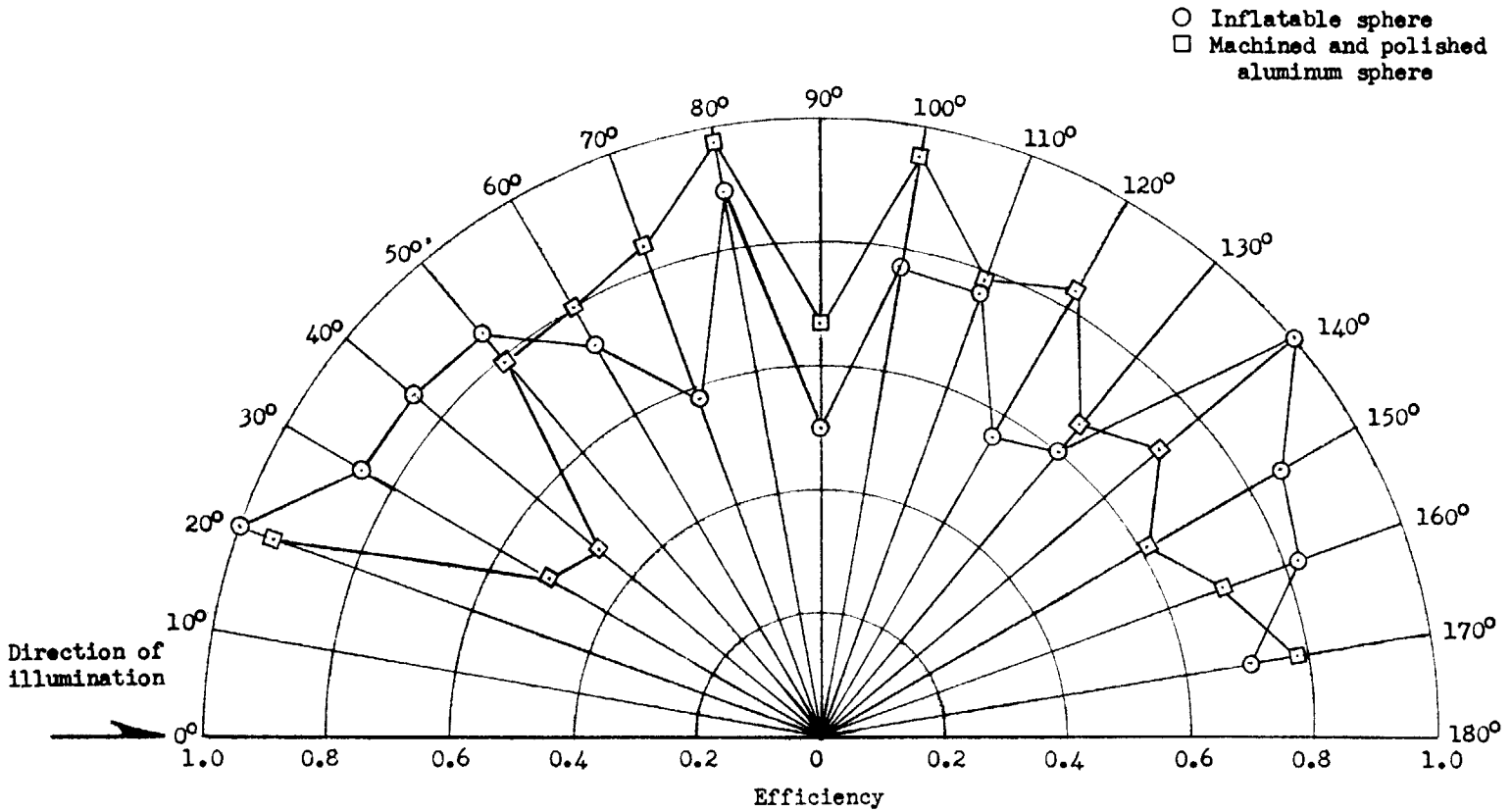

Figure 15.- Efficiency of a 4-inch-diameter inflatable sphere and a 4-inch-diameter machined and polished aluminum sphere.

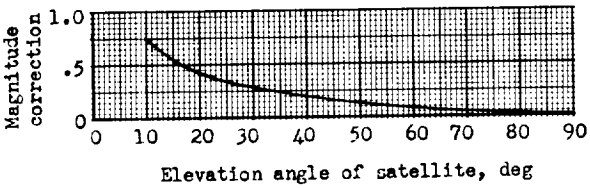

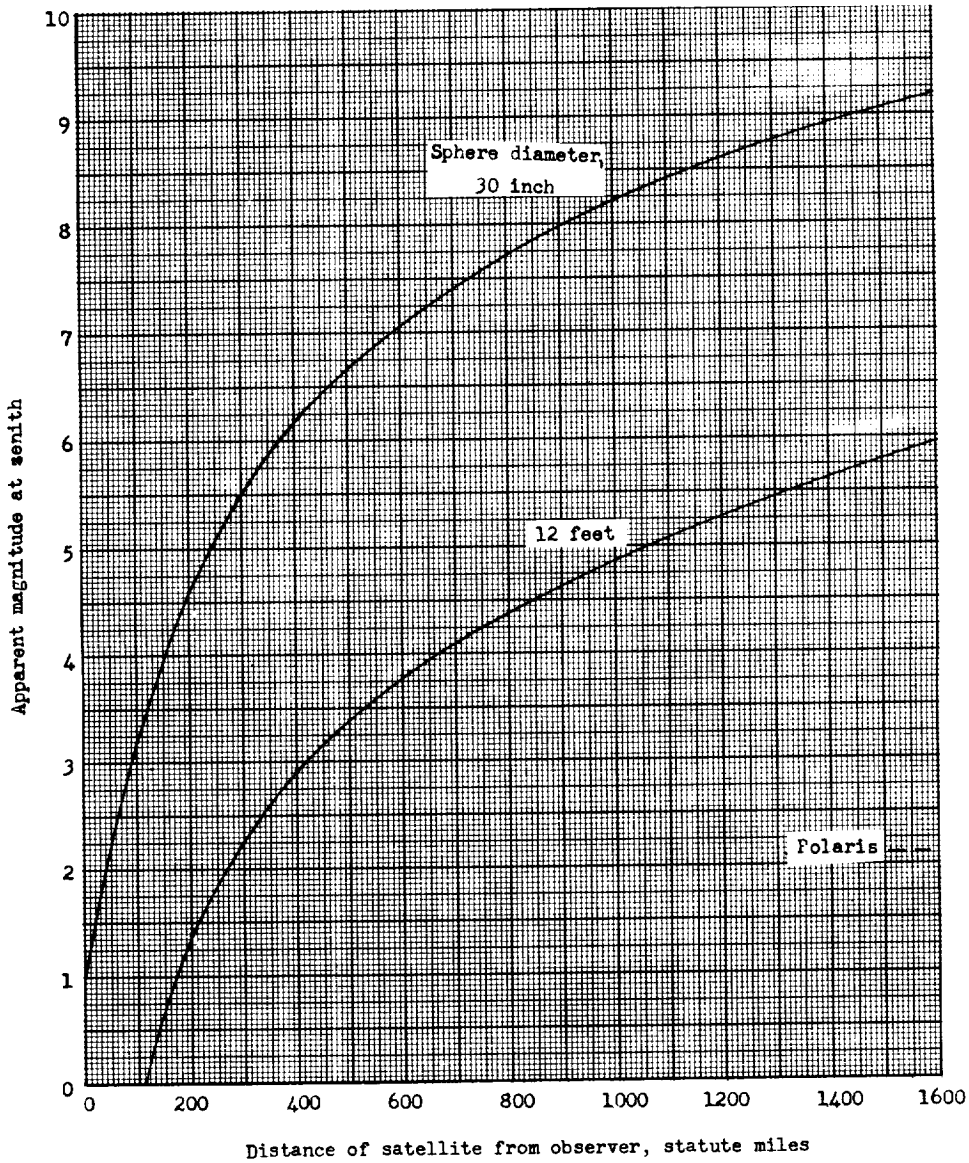

Figure 16.- Apparent magnitude at zenith for a specular, 79 percent reflectivity spherical satellite for a nighttime sky.

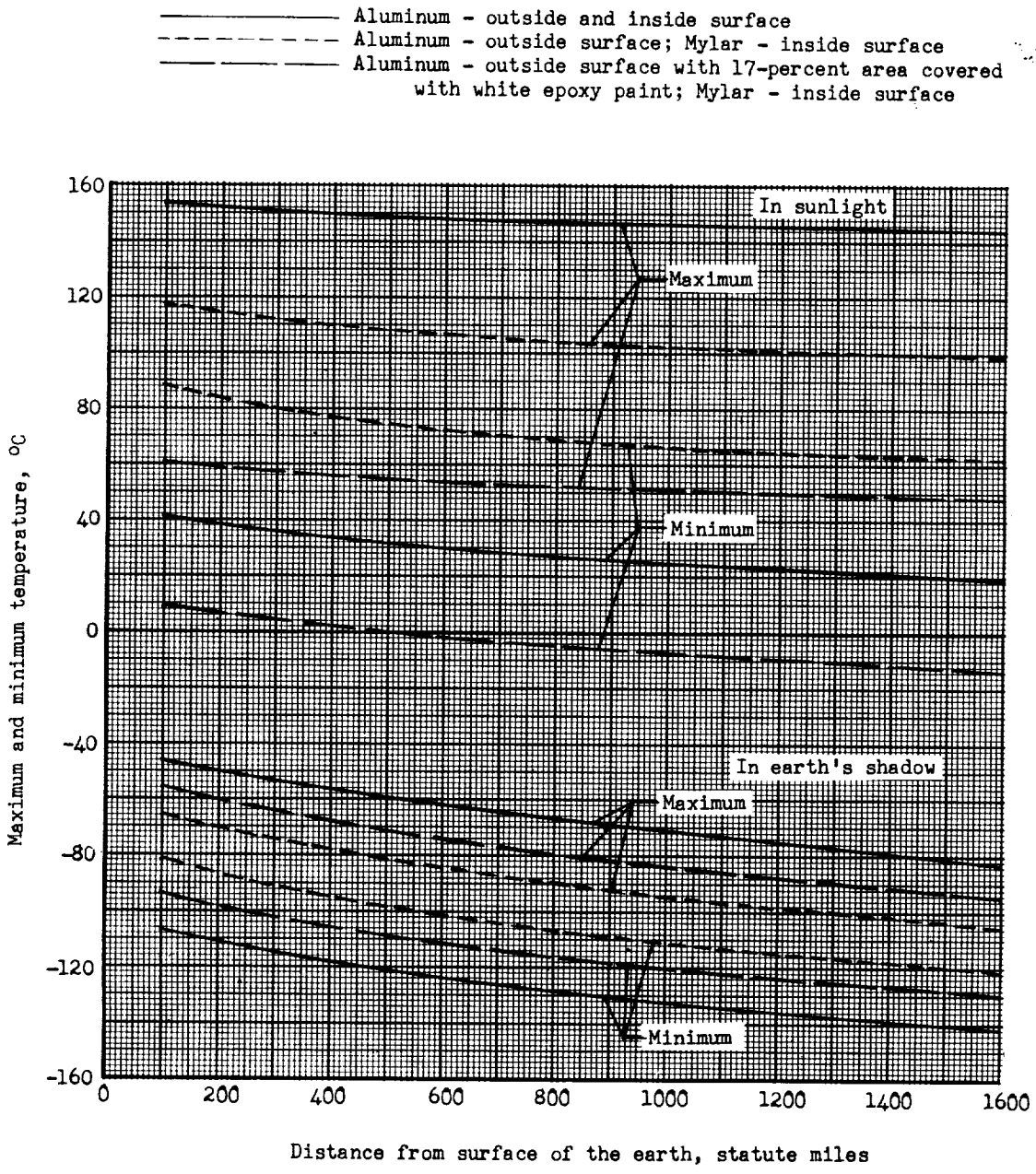

Figure 17.- Maximum and minimum temperatures on aluminum-plastic film inflatable spheres in satellite orbit.

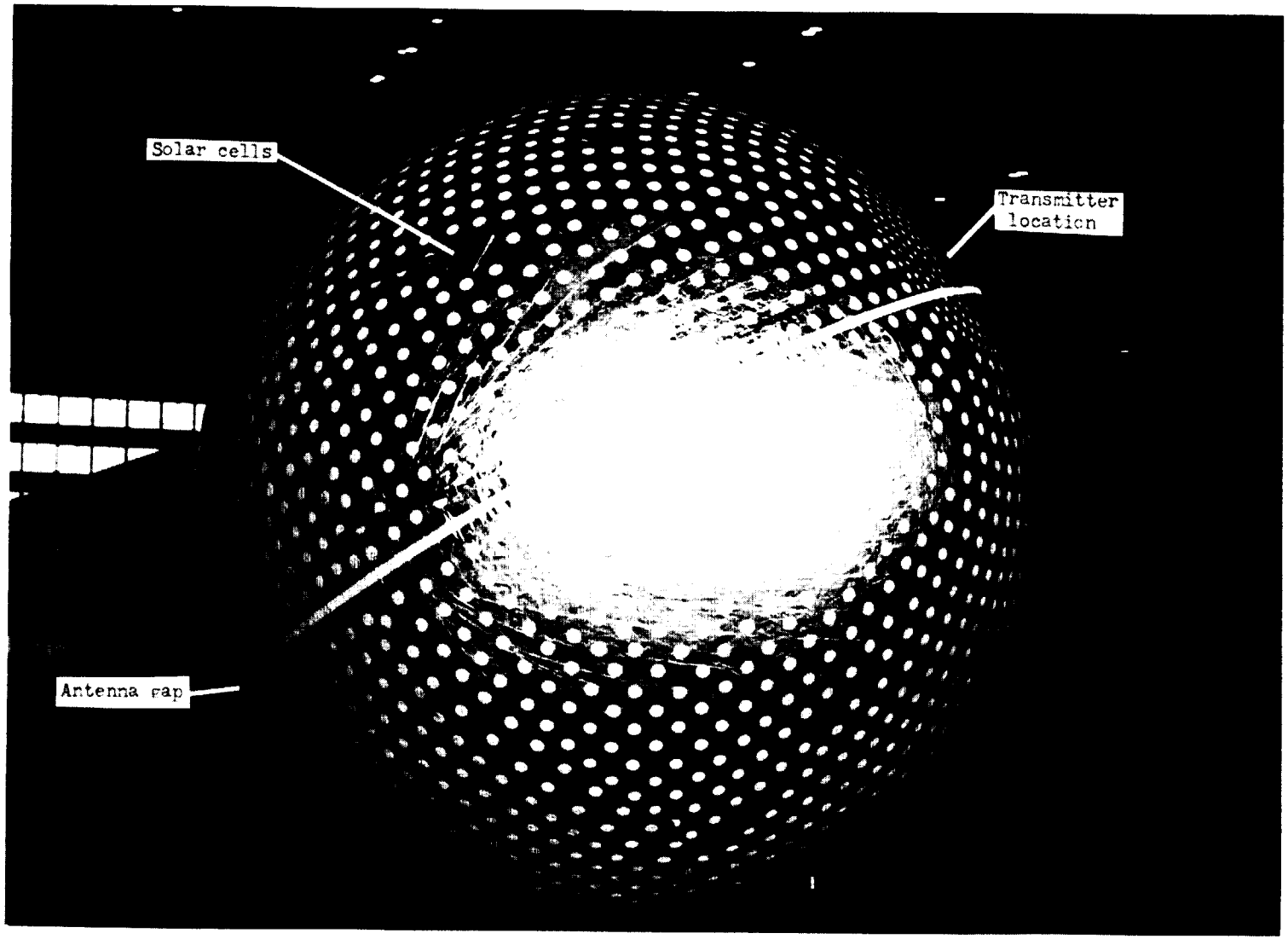

Figure 18.- Photograph of an Explorer IX satellite. L-61-3762.1

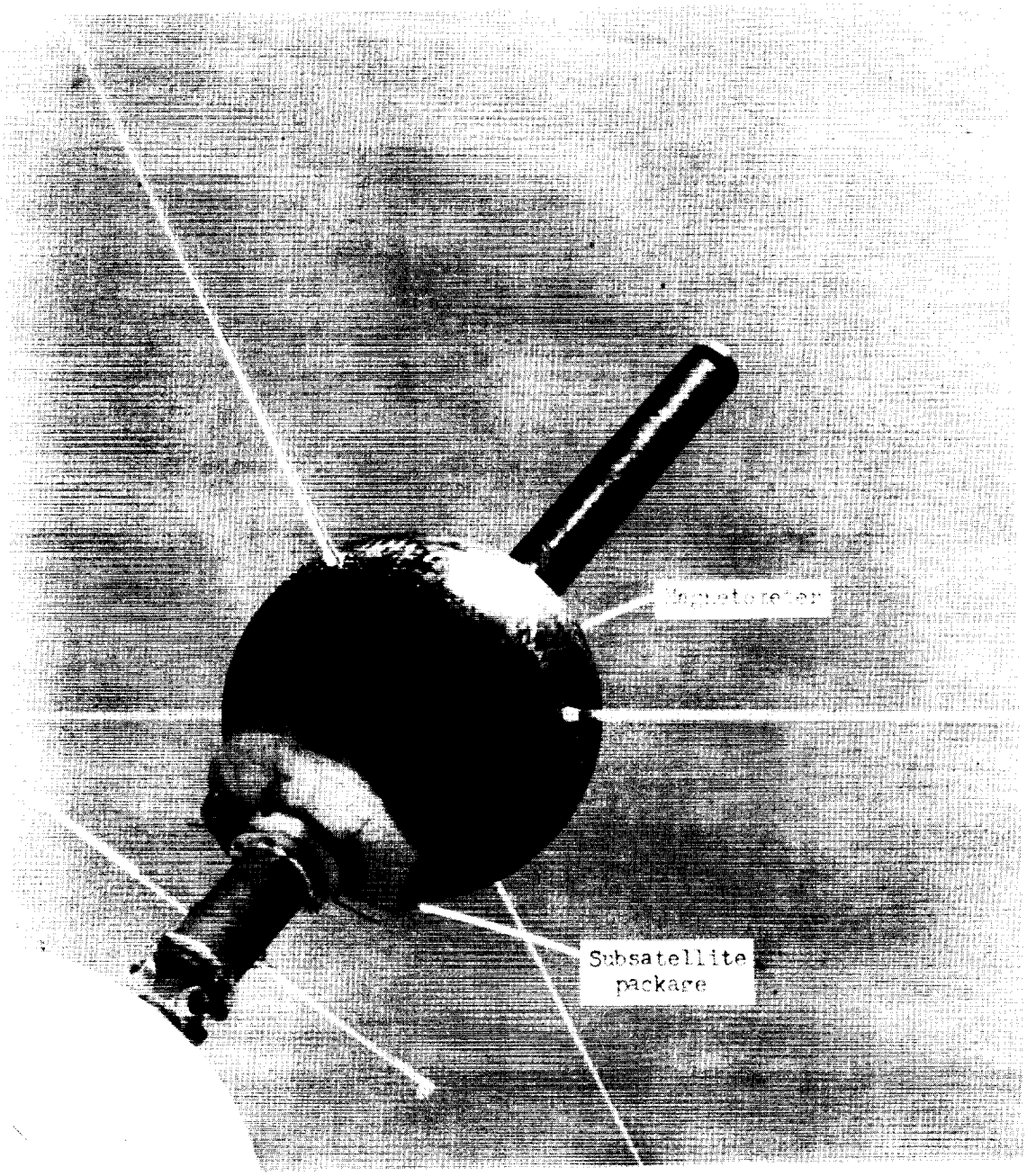

L-62-29

Figure 19.- Photograph of the arrangement of the packages on the last-stage vehicle.

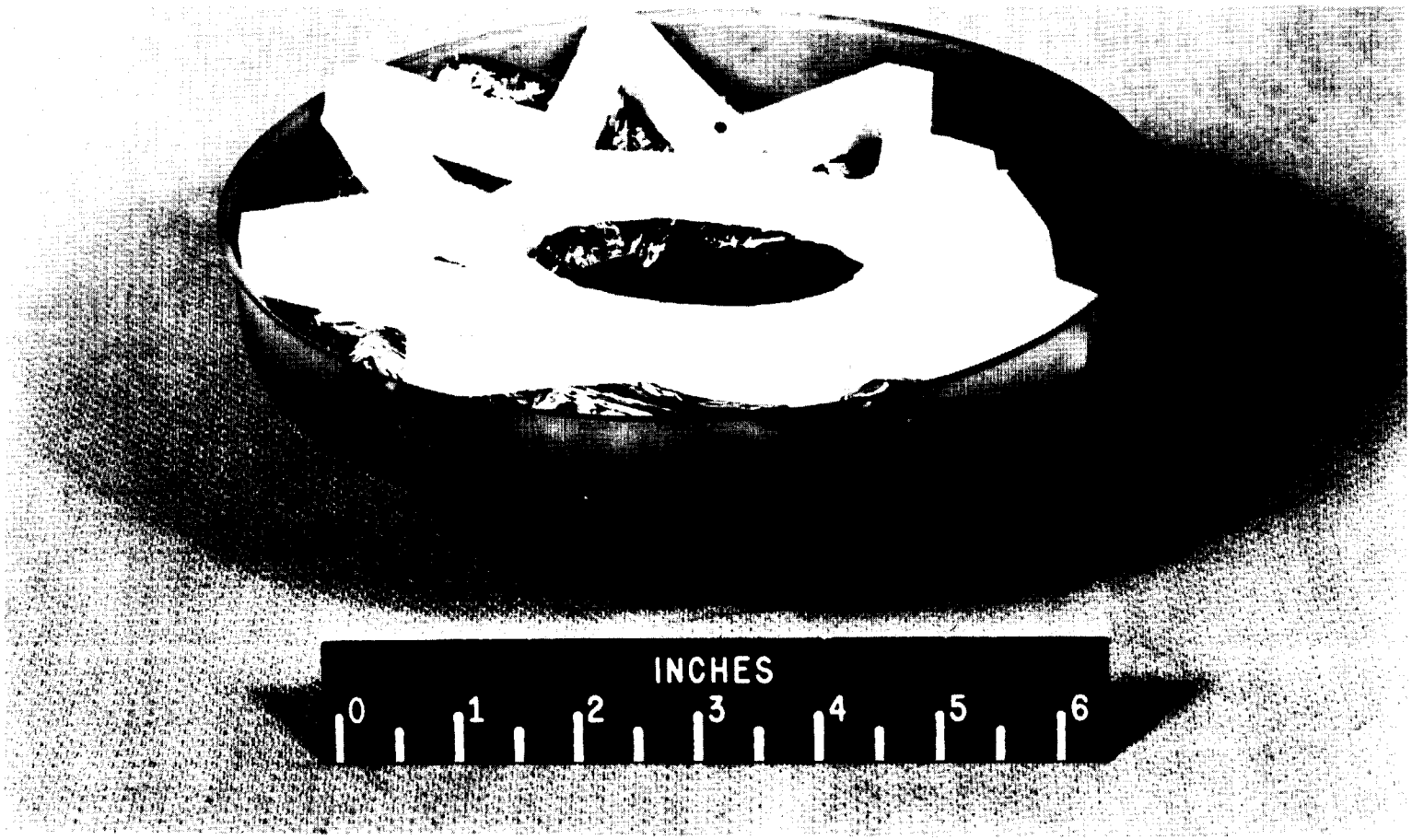

Figure 20.- Photograph of the 30-inch subsatellite package. L-59-2831

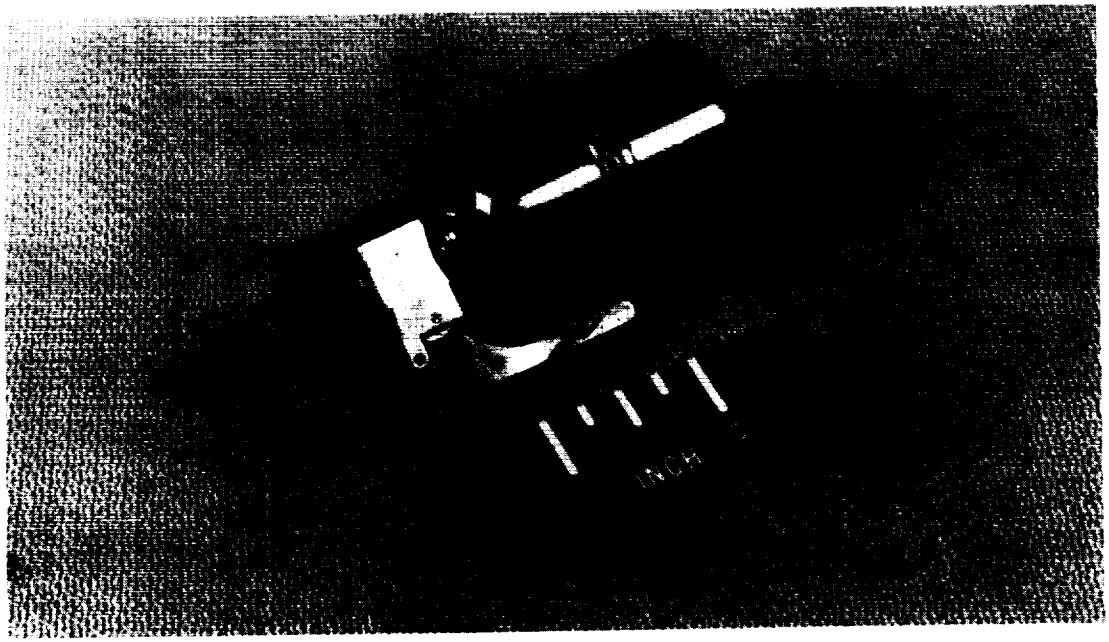

(a) Nondetachable bottle. L-59-2832

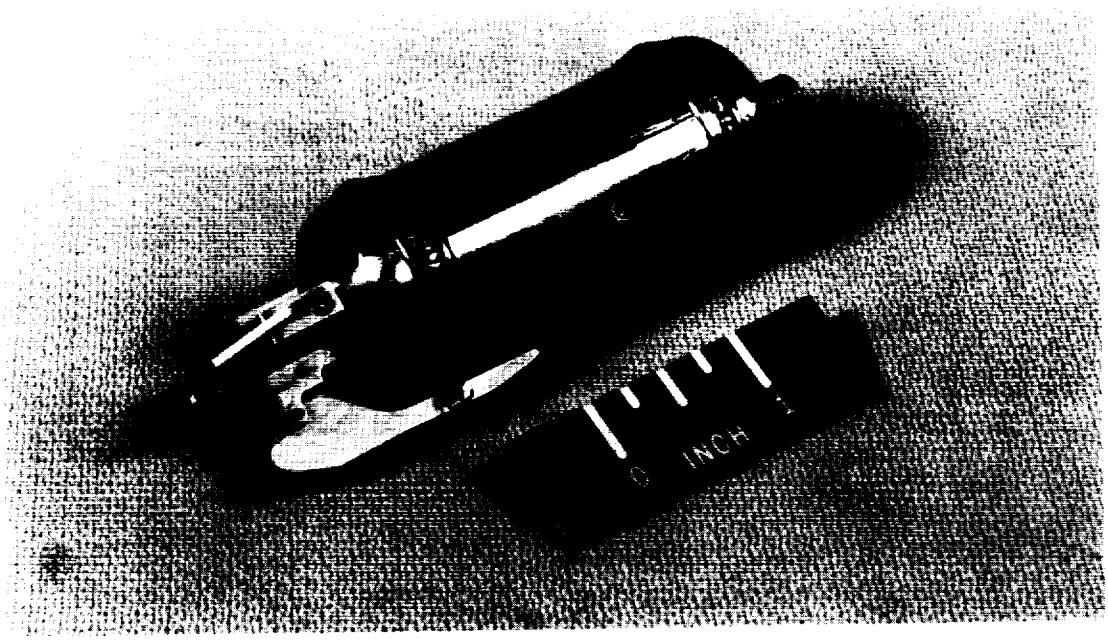

(b) Detachable bottle. L-59-2833

Figure 21.- Photographs of the inflation bottles designed for use with the 30-inch-diameter inflatable sphere.

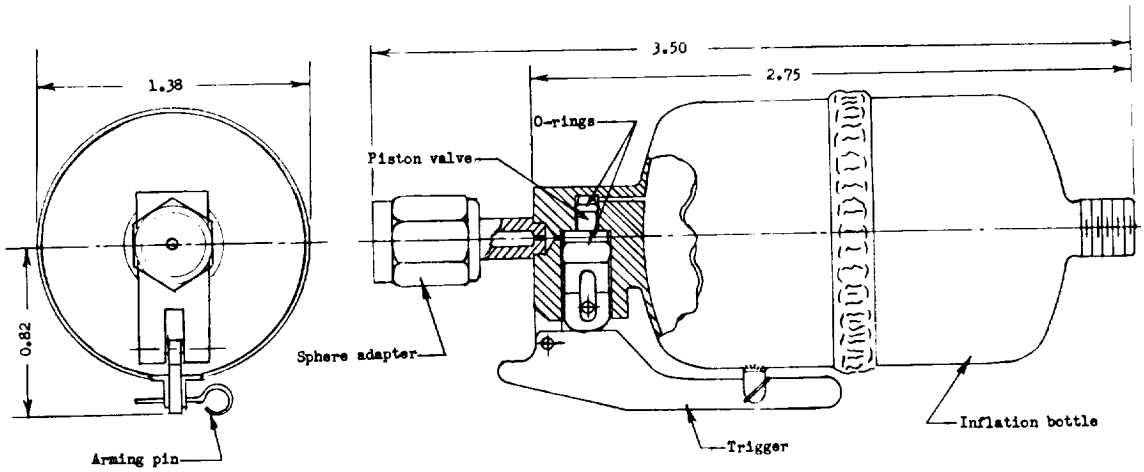

(a) Inflation-valve mechanism.

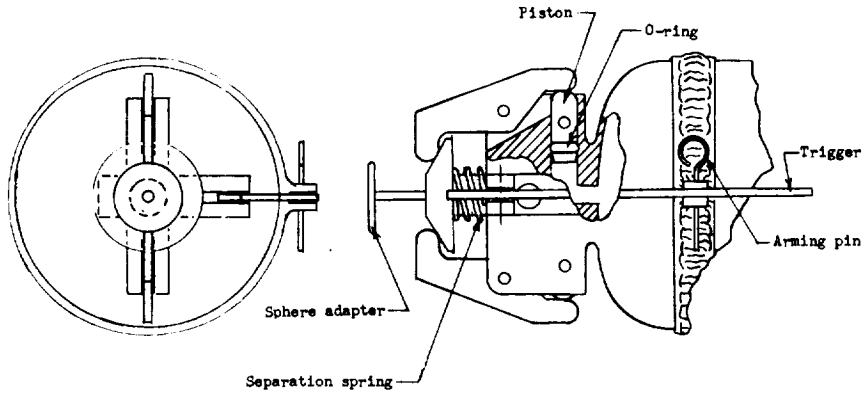

(b) Release mechanism for detachable bottle.

Figure 22.- Inflation bottle used with the 30-inch-diameter spheres.

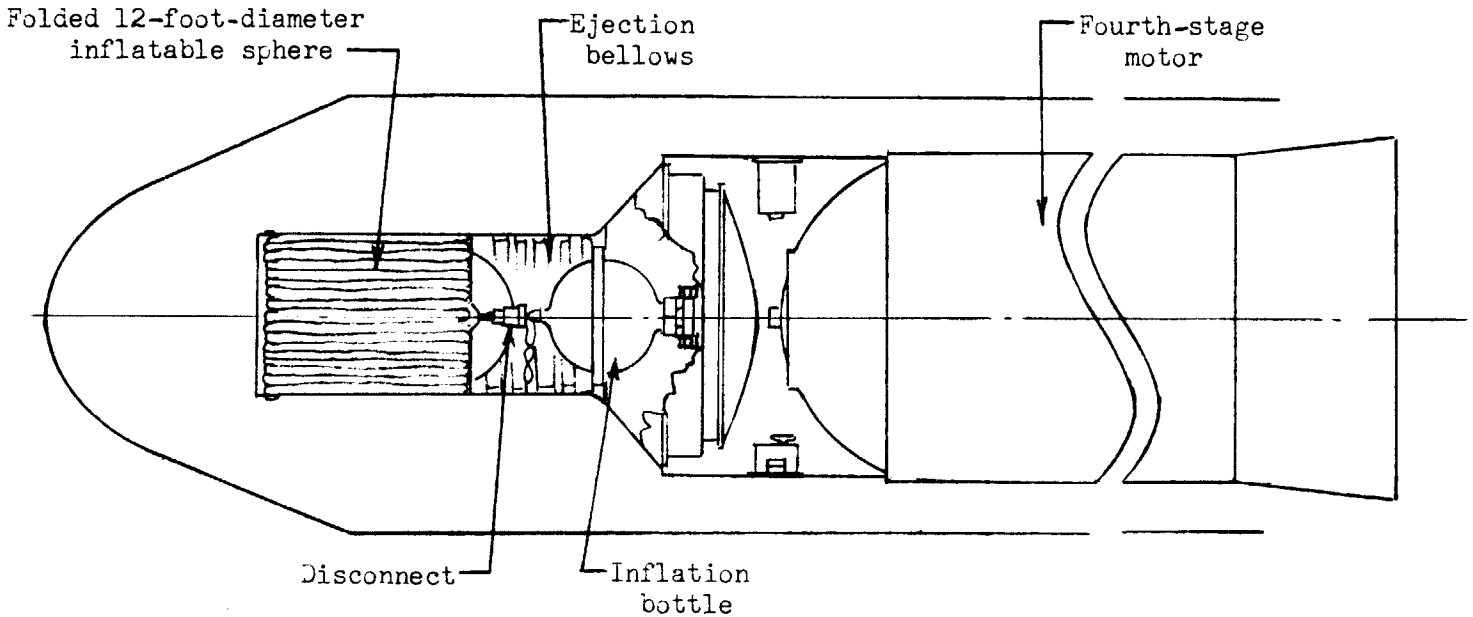

Figure 23.- Fourth-stage motor and payload assembly of the Scout payload package.

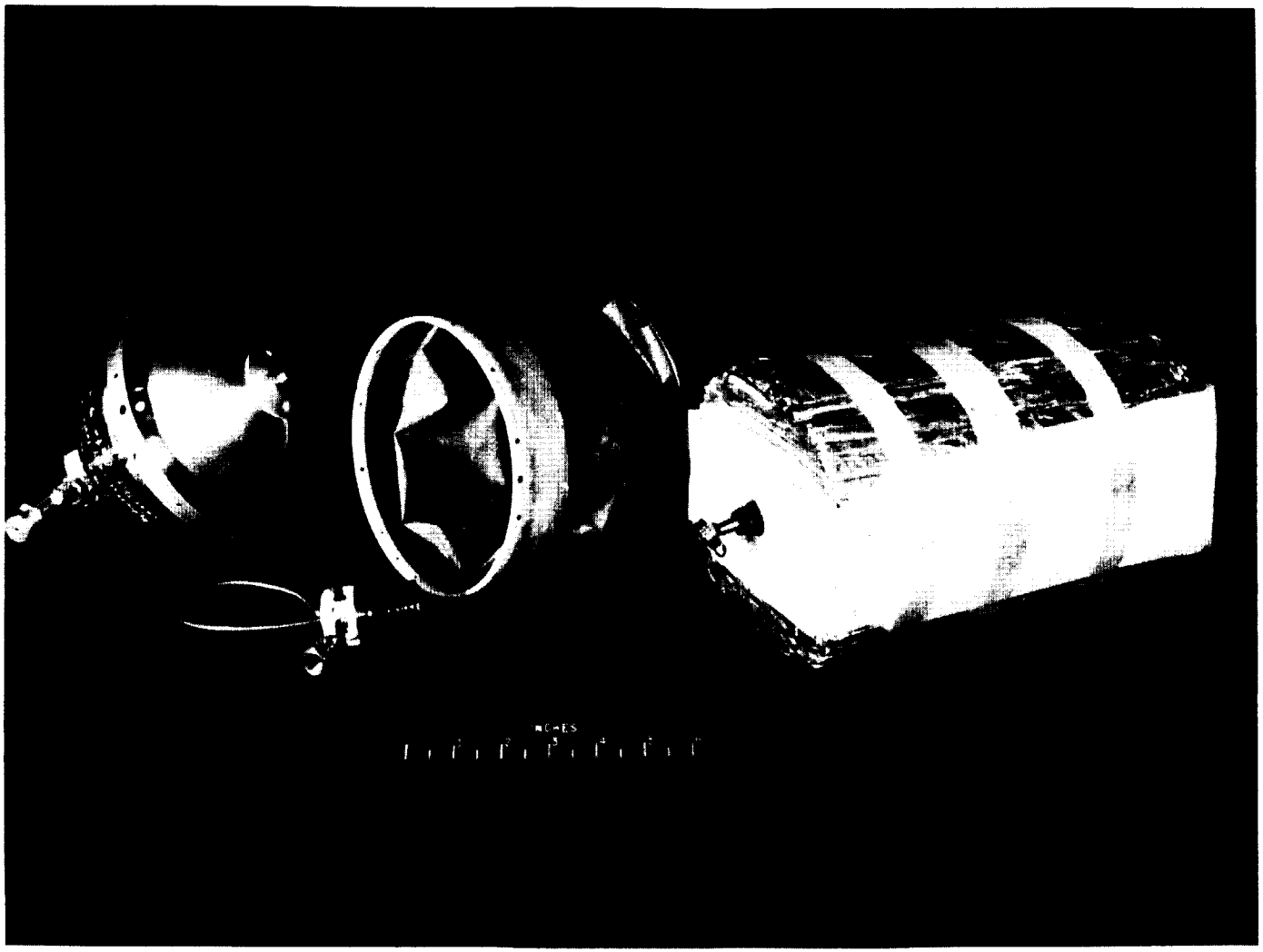

L-58-761a

Figure 24.- Photograph of the major subassemblies of the 12-foot-diameter inflatable sphere payload package.

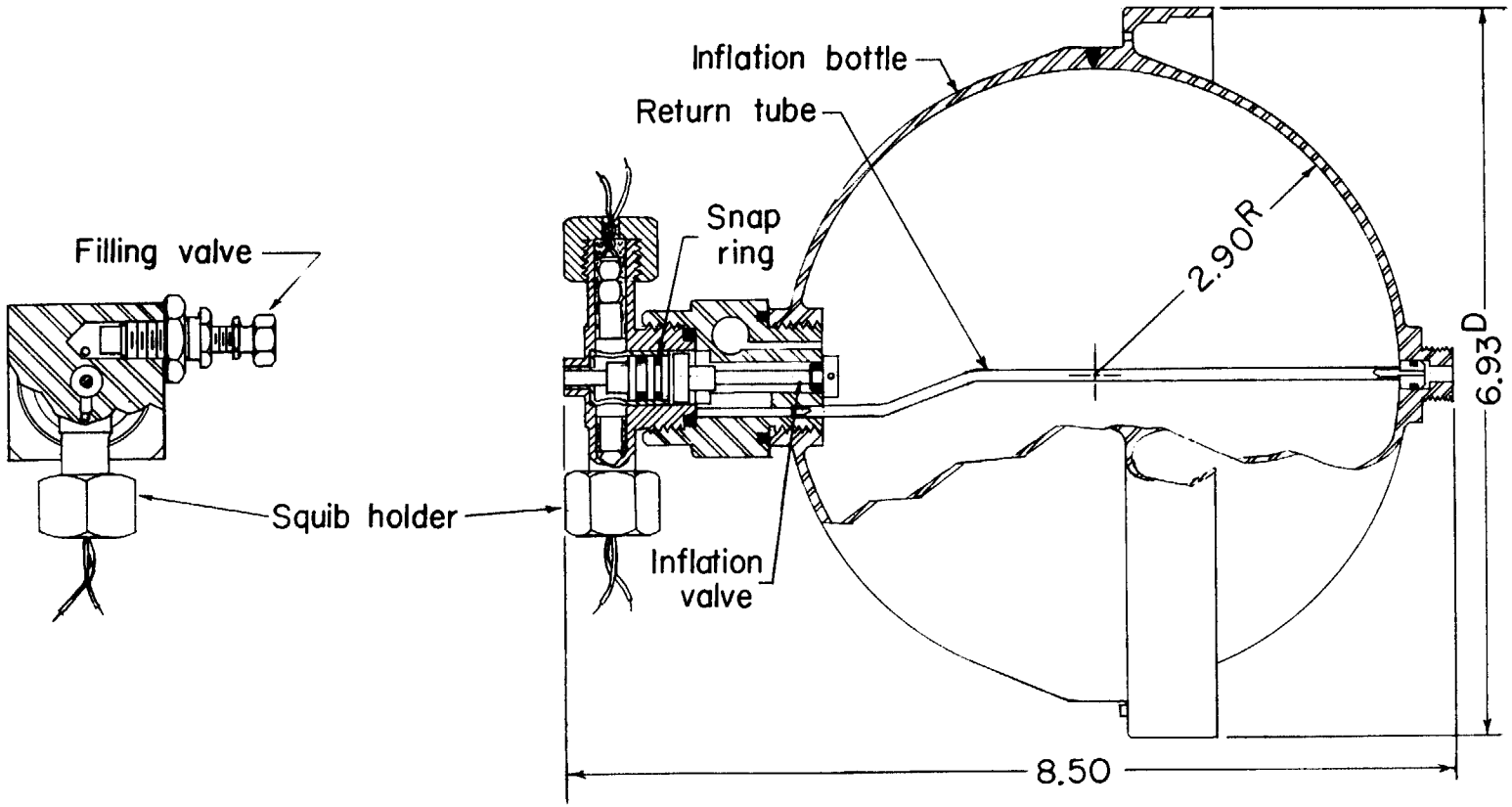

Figure 25.- Inflation bottle and valve mechanism used with the 12-foot-diameter inflatable sphere. (All dimensions are in inches.)

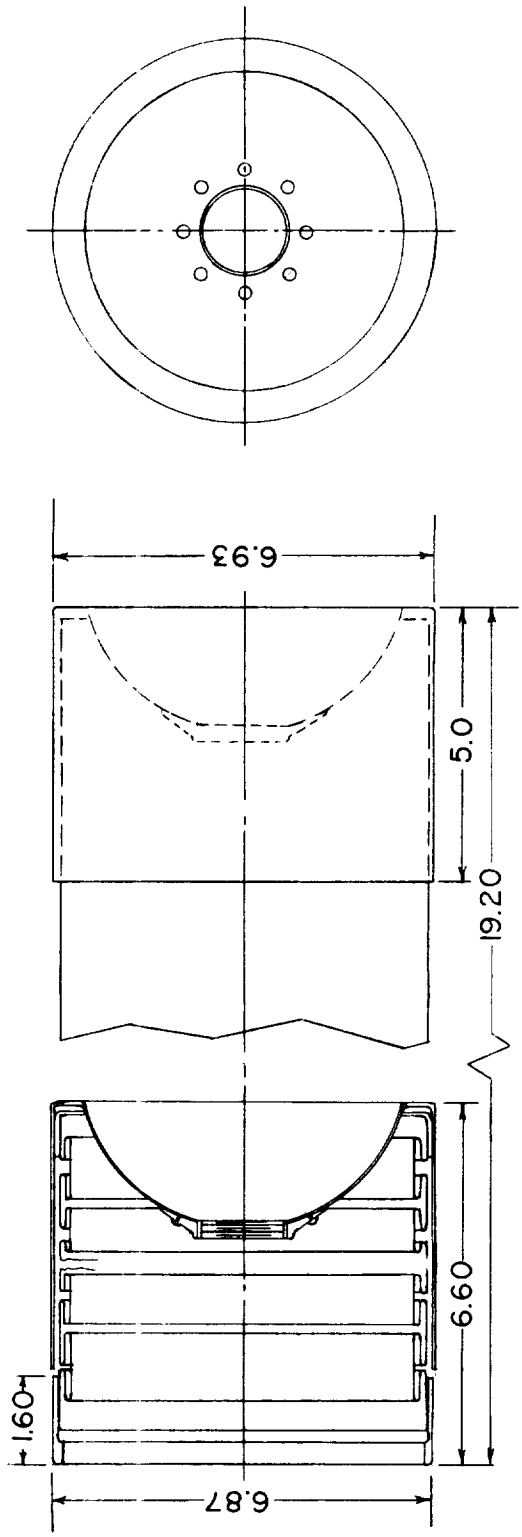

Figure 26.- Ejection bellows used with the 12-foot-diameter inflatable sphere. (All dimensions are in inches.)

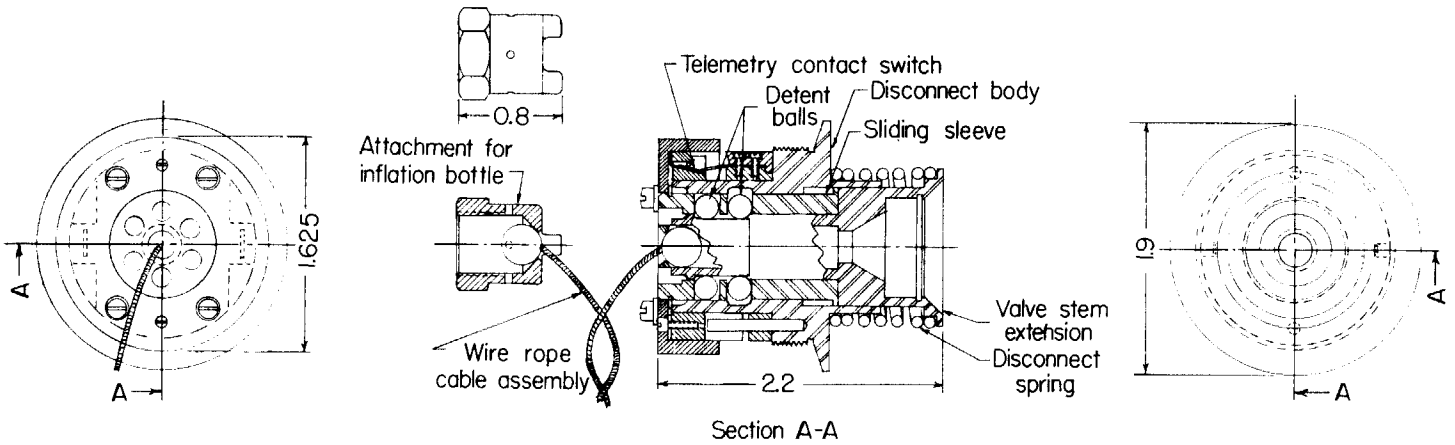

Figure 27.- Disconnect mechanism used with the 12-foot-diameter inflatable sphere.

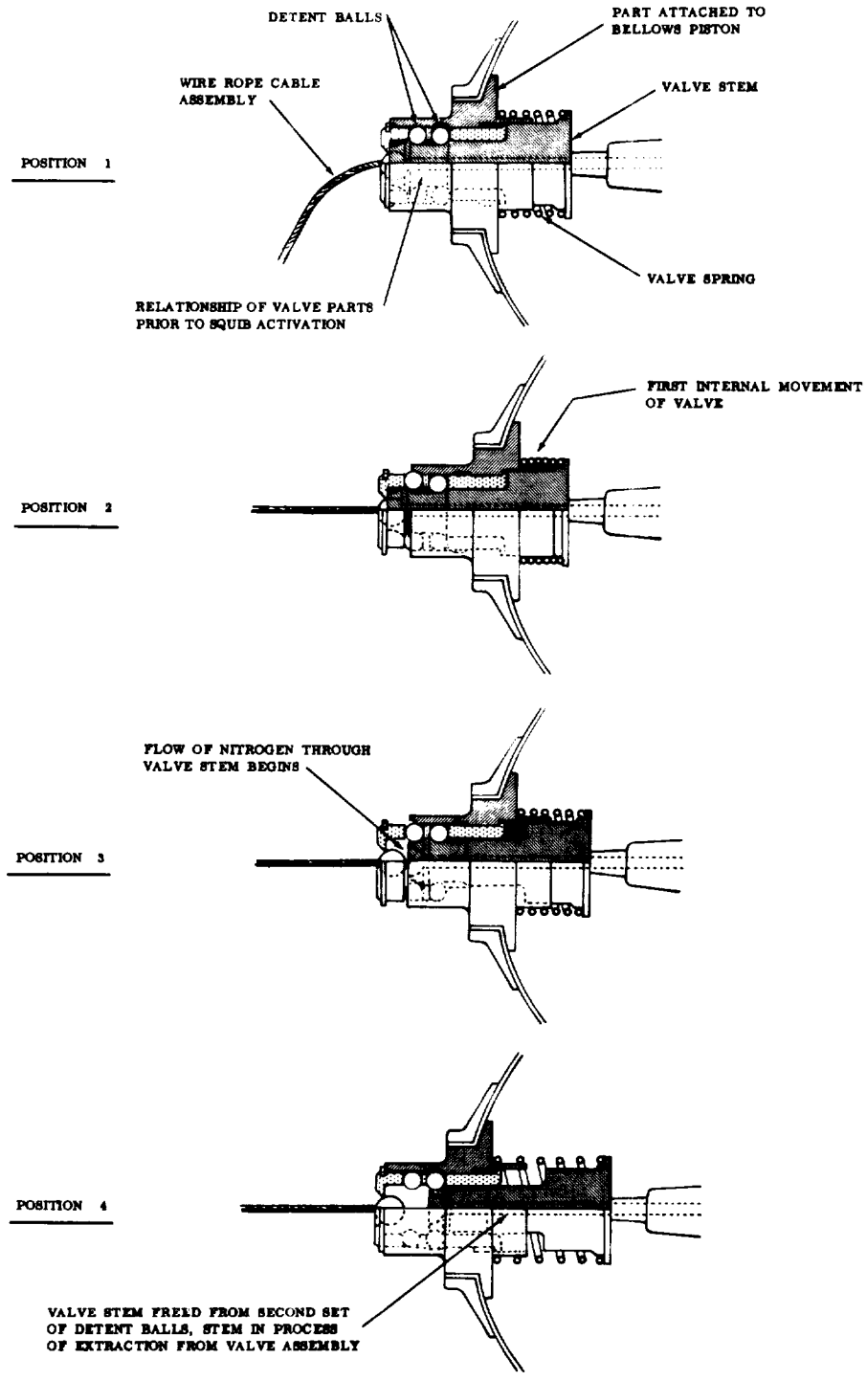

Figure 28.- Operational sequence of the disconnect mechanism.

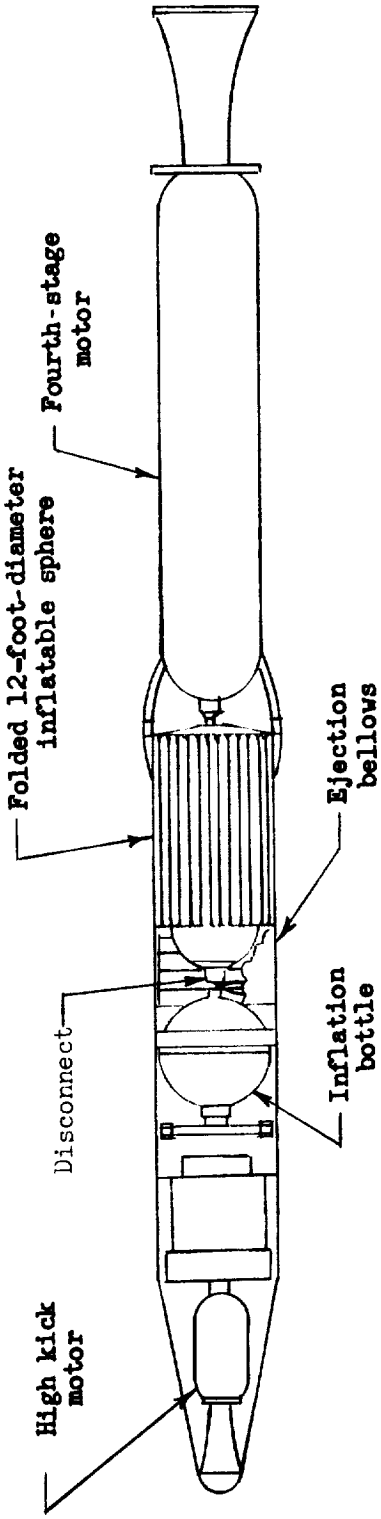

Figure 29.- Fourth-stage rocket motor and payload assembly of the Jupiter-C payload package.

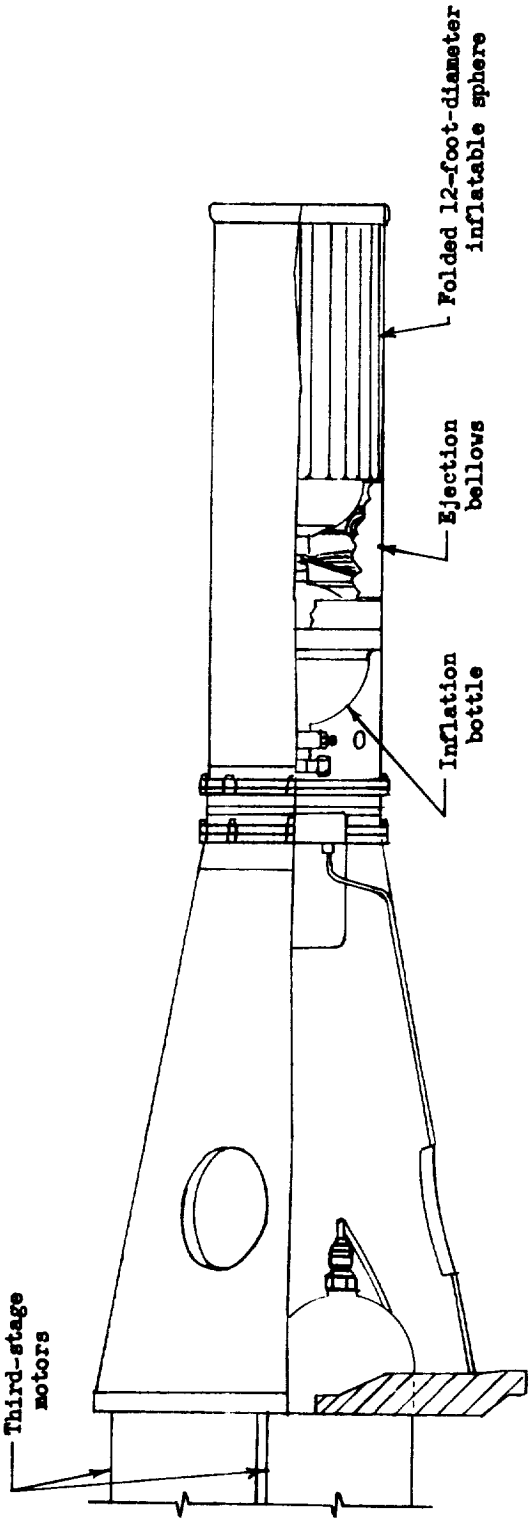

Figure 30.- Third-stage motors and payload assembly of the Juno II payload package.